International Journal of Heat and Mass Transfer 111 (2017) 467–483

Contents lists available at ScienceDirect

International Journal of Heat and Mass Transfer

journal homepage: www.elsevier.com/locate/ijhmt

Review

Summary and evaluation on the heat transfer enhancement techniques of gas laminar and turbulent pipe flow

Wen-Tao Ji [a,b,*], Anthony M. Jacobi [b], Ya-Ling He [a], Wen-Quan Tao [a]

[a] Key Laboratory of Thermo-Fluid Science and Engineering of MOE, School of Energy and Power Engineering, Xi'an Jiaotong University, Xi'an, China
[b] Department of Mechanical Science and Engineering, University of Illinois at Urbana-Champaign, Urbana, IL, USA

ARTICLE INFO

Article history:
Received 10 December 2016
Received in revised form 21 March 2017
Accepted 22 March 2017
Available online 12 April 2017

Keywords:
Turbulent
Heat transfer enhancement
Pipe flow
Performance evaluation

ABSTRACT

A systematic survey and evaluation on the thermal-hydraulic performance of gas inside internally finned, twisted tape or swirl generator inserted, corrugated, and dimpled, totally 436 pipes is conducted in this work. The gases in the investigations involve air, nitrogen, exhaust gases, and helium. Prandtl number is around 0.6–0.7. It is found that in the Reynolds number of 2×10^3 to 100×10^3, the ratios of Nusselt number over Dittus-Boelter equation for internal finned tubes are typically in the range of 1–6, tubes with twisted tape and other inserts are 1.5–6, corrugated tubes are 1–3 and dimpled tubes are 1–4, including compound enhancement techniques. The ratios of friction factor over Blasius equation is normally in the range of 1.5–14 for internally finned tubes, 2–200 for inserted twisted tapes and swirl generators, corrugated tubes is 1.5–10 and dimpled tubes is 1–8. The heat transfer enhancement ratios for gases are generally similar with liquid, while the friction factor increased ratios for gases are higher than that for liquids. The number of investigations on the tubes fitted with twisted tapes inserts, coil loops, and swirl generators are more than other three enhancement methods. The increment of pressure drop for twisted tape inserts are also the largest. By using performance evaluation plot, different enhancement techniques with the same reference are compared for their effectiveness. It indicates that the efficiency of pipes with different types of inserts for gases are mostly lower than internal finned, corrugated and dimpled tubes in this survey.

Contents

* Corresponding author at: Key Laboratory of Thermo-Fluid Science and Engineering of MOE, School of Energy and Power Engineering, Xi'an Jiaotong University, Xi'an, China.
E-mail address: wentaoji@xjtu.edu.cn (W.-T. Ji).

http://dx.doi.org/10.1016/j.ijheatmasstransfer.2017.03.080
0017-9310/

Nomenclature

A_n	nominal heat transfer area based on the internal diameter as if the fin structure were not present, m^2
A_a	actual heat transfer area, m^2
A_{fa}	actual flow area, m^2
A_{fc}	core flow area through an internally finned tube ($A_n(1-H)^2$), m^2
A_{fn}	nominal flow area based on the internal diameter as if the fin structure were not present, m^2
A_{fin}	inner fin flow area through an internally finned tube, m^2
b	half of the fin spacing, m
$\overline{B}(e^+,\alpha)$	friction factor correlating parameter for helical-rib roughness, dimensionless
$\overline{B}(e^+)$	friction factor correlating parameter for geometrically similar roughness and friction similarity function, dimensionless
d_i	internal diameter of tube, m
d_h	hydraulic diameter, m
e^+	roughness Reynolds number $(e/d_i)Re(f/2)^{1/2}$, dimensionless
e	absolute roughness (fin height), m; Fin height on the twisted tapes, m
Gr	Grashof number, $g\rho^2 d_i^3 \beta \Delta T_w/\mu^2$, dimensionless
$\overline{g}(e^+)$	heat transfer correlating parameter for geometrically similar roughness, dimensionless
H	non-dimensional fin height ($2e/d_i$), pitch for 180-deg rotation of tape, dimensionless
n	index of Prandtl number in Dittus-Boelter equation
N_s	number of fins
Nu	Nusselt number
p	Rib pitch ($\pi d_i/N_s$), m
p_i	fin pitch based on fin tip diameter, m
ΔP	pressure drop, Pa
t_b	fin base thickness, m
u	fluid velocity, m/s
w	tape width, m
y	twist ratio, $y = H/w$
α	Helix angle, degree (°)
ν	kinematic viscosity, m^2/s
ϕ	Chamfer angle in [22], degree (°)
λ	thermal conductivity, W/m K
δ	tape thickness, m
ρ	fluid density, kg/m^3
μ	fluid dynamic viscosity, $(N\,s)/m^2$
τ	apparent wall shear stress, $\tau_o = -\frac{d_i dP}{4dx}$

Subscripts

c	corrugated tube
d	dimpled tube
f	fluid or internally finned tube
s	smooth tube
r	reference
t	tape inserts
w	tube wall

1. Introduction

The encouragement and requirement to fabricate ultra-compact heat exchangers have driven the development of many types of surfaces to enhance the heat transfer. Because heat transfer enhancement of gases usually needs large surface area and the intensification from tube side is limited by space, the enhancement techniques typically locate in outside of tubes. However, although the heating or cooling of gas through internal tubes are not as prevalent as that in outside, there are still many applications in industry involving the heat transfer enhancement of gas laminar and turbulent pipe flow. The examples include compressor intercooler, solar air heaters, waste heat recovery from high temperature flue gas, gas turbine regenerator, heat transfer of natural gas in liquefier and vaporizer, earth or solar to air heat exchanger [1,2]. The methods to augment the heat transfer in tube-side usually involve extended surfaces such as internal fins, twisted tape inserts, corrugations and three dimensional roughness or protrusions.

Compared with pipe flow of liquid, gas has its unique characteristics. The thermal properties like Prandtl number, thermal conductivity, density, and specific heat capacity are quite different from liquid. Typically, air-side thermal resistance might constitute more than 80% of the total thermal resistance for heat transfer. Air-side heat transfer usually plays a critical role in the overall thermal resistance. Because there are many factors which can influence thermal-hydraulic performance, the heat transfer enhancement techniques and mechanisms of enhancement for gas might be different from liquid. Prandtl number of air is generally in the range of 0.6–0.7. Thermal conductivity is quite small, mostly within 0.05 W/m K [3,4]. The Prandtl number and thermal conductivity of water at 20 °C is as much as 10 times higher than air. Thus, the heat transfer coefficient of water should be higher than air more than one order of magnitude.

As gas-side thermal resistance is the most influential factor in overall heat transfer process, the heat transfer enhancement of that should contribute the most to the efficiency of heat exchanger. Many investigations were conducted to test the hydraulic and thermal performance of gas pipe flow. A systematic survey on the heat transfer of air turbulent flow inside internally finned tube was conducted by Webb et al. [5]. The parameters of fins and fluid are $0.01 < e/d_i < 0.04$, $10 < p/e < 40$, and $6000 < Re < 130{,}000$. Experimental results indicated that the improvements in heat transfer coefficients for internally finned tube (based on nominal surface area) were 250%. However, pressure drops are as much as 7–13 times higher.

The enhancement techniques for gases include integral-fins, inserted devices like twisted tapes and coils, swirl generators, corrugated or twisted tubes, dimpled or integral roughness and other three dimensional protrusions, which all have been used to improve heat transfer in both laminar and turbulent flow. Each technology has its unique features and the in-detail survey may

invite new ways of looking at this problem. It might also aid to the evolution of heat transfer enhancement technologies for pipe flow. In this paper, the correlations and experiment result regarding the heat transfer of gases, mostly air, are systematically summarized. The most commonly used techniques are reviewed and compared.

Another paper reported by the same authors is on the summary and evaluation of liquid laminar and turbulent pipe flow heat transfer [6]. The primary features of liquid flow heat transfer enhancement techniques were evaluated and analyzed in this paper. These enhanced techniques were also used for pressurized gases, while the heat transfer and flowing resistance features are quite different. The enhancement techniques can also be roughly classified into the above mentioned four categories. The techniques belonging to the same type might behave similarly both in pure laminar and turbulent regimes. The summary and comparison on both liquid and gas can provide detailed insight into the effect of thermodynamic and fluid dynamic on the heat transfer of different enhancement techniques.

It is a quite well-known fact that any enhancement technique is accompanying an additional frictional loss, and usually the ratio of frictional loss increase is larger than that of heat transfer. However, the optimization of heat exchangers is always directed to maximize the heat transfer and minimize the pressure loss. Hence it is very important to quantitatively identify the overall thermo-hydraulic performance of a given enhancement technique. In order to determine which types of enhancement techniques has a higher efficiency for fluids, Fan et al. [7] proposed a performance evaluation method to evaluate the thermo-hydraulic performance of enhanced techniques. In the evaluation plot, $\lg(Nu_e/Nu_r)$ and $\lg(f_e/f_r)$ are taken as the ordinate and abscissa, respectively. The increase of heat transfer and friction factor are presented and compared simultaneously. By using this performance evaluation criteria, the highest heat transfer enhancement and the minimum increase of pressure drop can both be observed. Every enhancing parameters can be expressed in the figure and under what constraint the technique will enhance heat transfer can be clearly identified. For simplicity of presentation the assumptions and details of plot [7] are omitted here. It can be confirmed that all the techniques and related test data compared in this paper satisfy the assumptions made in [7]. The comparison and evaluation for enhanced tube and reference plain tube are based on the same internal diameter(d_i).

In the following presentation, it is divided into five sections: internally finned tubes are reviewed and evaluated in Section 2; Section 3 is for twisted tape, coiled loops and other swirl promoter inserted tubes. In Section 4, corrugated and twisted tubes are presented; dimpled and the tube with internal three dimensional protrusions are summarized in Section 5; and finally, some conclusions are made in Section 6.

2. Internally finned tubes

2.1. Introduction of internally finned tubes

As reported in the literature [6,8–12], internally finned tubes are produced by rolling, machining, casting, or welding. A certain number of protruding fins is spirally or vertically extruded from the internal tube wall, which creates an extended surface to the inner tube for more area and greater heat transfer capability. The cross section of fin can either be rectangle, triangle or trapezoid. The attached fins like louvered fins, perorated fins, or corrugated fins were also used for heat transfer enhancement of gases. The pressure drop might be pretty high for the fins with narrow space. The photos and schematic diagrams are shown in Figs. 1 and 2. As depicted in Fig. 2, the geometric parameters of finned tube include the internal diameter of tube(d_i), inner fin height(e), number of starts(N_s), helix angle (α), fin base thickness (t_b), and fin pitch (p, $\pi d_i/N_s$).

Compound technique involves at least two of above mentioned enhancement methods. It is assumed that the heat transfer could be further augmented with a combination of any two or more of the enhancement techniques. However, the pressure drop may also substantially increase with the compound methods. The combination is usually the inserted device and finned, corrugated or three dimensional roughed tubes. The increment of friction factor is usually higher for compound techniques [13].

2.2. Correlations for average heat transfer coefficient and friction factor

For more than fifty years, investigators have been seeking to understand and develop an accurate prediction method for different roughness geometry and pick up the best performed tubes for heat exchangers. Although it has been largely empirical, many of correlations regarding the heat transfer and friction for the pipe flow of gas have been proposed based on analytical solution or experimental result. Normally, different geometrically similar enhancement techniques cannot be correlated with a single correlation. The correlations for gases are compiled in Table 1. The correlation might involve a constant or variable gas compressibility factor.

The equations listed in Table 1 can be broadly classified into two main categories. Some involves transformations of Nikuradse [14] and Dipprey and Sabersky [15]'s analytically based models. Others are empirically based correlations.

One of the earliest predictions of friction factors for tube with internal roughness was firstly established by Nikuradse [14].

$$\overline{B}(e^+) = \sqrt{2/f} + 2.5ln(2e/d_i) + 3.75 \tag{1}$$

where e^+ is roughness Reynolds number, $e^+ = \frac{eu^*}{\nu} = \frac{e\tau_w/\rho}{\nu} = (e/d_i)Re\sqrt{f/2}$. $\overline{B}(e^+)$ is a friction similarity function determined empirically by the shape of each roughness type, which is a constant 8.48 when e^+ is more than 70.

Dippery and Sabersky [15] developed a more general heat transfer similarity correlation for smooth and roughed tubes. It is complementary with Nikuradse's friction similarity law. The correlation is written in the following form:

$$Nu = \frac{(f/2)RePr}{1 + \sqrt{f/2}\left[\overline{g}(e^+)Pr^n - \overline{B}(e^+)\right]} \tag{2}$$

$\overline{g}(e^+)$ is a dimensionless heat transfer similarity function. $\overline{g}(e^+)$ can be determined from a new set of experiments for each type of roughness. It is assumed that this law of wall similarity might be applicable to any arbitrary types of roughness, and the prerequisite is friction data for any geometrically similar forms of roughness should be correlated.

Based on the studies of Nikuradse [14], and Dipprey and Sabersky [15], Webb et al. [5] developed a generalized correlation for Nusselt number and friction characteristics of geometrically similar finned tubes with $0.7 \le Pr \le 37.6$. The correlations of Han [16], Kader and Yaglom [17], Gee and Webb [18], Kim and Webb [19] listed in Table 1 are also basically derived from Eqs. (1) and (2).

In Table 1, friction factor and Nusselt number are also described as a function of dimensionless parameters (Reynolds number (Re), Prandtl number (Pr)), and geometric parameters (e/d_i, p/d_i, helix angle (α), number of starts per circle (Ns), flow or heat transfer area) based on experimental measurements. Such correlations provide reasonable results in their range of applicability and can be

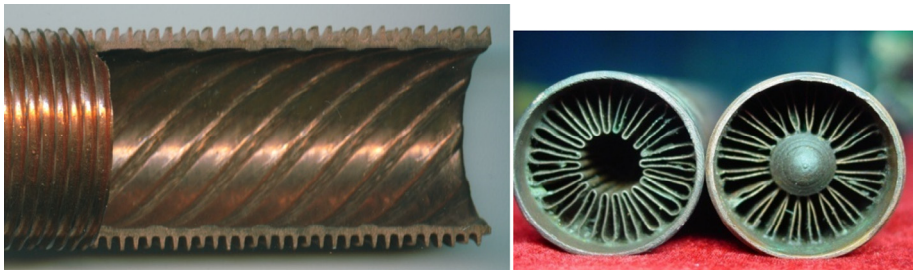

Fig. 1. Internal finned tubes.

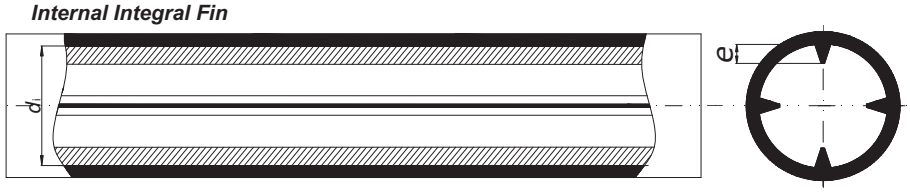

Fig. 2. Schematic diagram of internally finned tubes.

implemented without much difficulty. The heat transfer and pressure drop data were also correlated based on experimental data of 11 tubes by Carnavos [20]. The correlating equations for heat transfer and friction factor could describe air, water, and ethylene glycol-water data within ±10%. Experimental data of Ravigururajan and Bergles [21] were from the referred investigations with Reynolds number from 5000 to 250,000 and Prandtl number from 0.66 to 37.6. Other parameters include: $1 \leq Ns \leq 45$, $0.01 \leq e/d_i \leq 0.2$, $0.1 \leq p/d_i \leq 7$, $0.3 \leq \alpha/90 \leq 1$. The data were applied to a linear model to obtain normalized correlations among variables similar with smooth tubes. The correlations developed by Layek et al. [22] were also from regression of experimental data.

It should be noted that modeling of fluid flow and heat transfer inside the internally finned tubes is not simple, which involves sophisticated analytical techniques, simulations and a large number of experimental validations. The equations listed in Table 1 is largely verified by limited experimental results and extrapolation of such correlations may not yield good predictions because it might be suitable for the parameters only within the scope of their development.

2.3. Experimental measurements

Although the aforementioned correlations can reasonably well predict the heat transfer and friction factors within a wider range. Qualitative review and performance comparison on the original test data is also very important and accurate. By using comprehensive performance evaluation method, the heat transfer and flow friction can both be considered. The experimental data on the heat transfer of gas inside internally finned tubes from 1971 to 2016 are collected to the best of the author's knowledge in this section.

In Table 2, experimental studies on the heat transfer of gases inside internally-finned tube with different geometrical parameters from literature are summarized. It should be noted that more than 90% of experimental data of plain tube in the survey agree with Dittus-Boelter and Blasius equations within ±20%. Thus it can be confirmed the following comparisons are based on the same references in the comparison and evaluation.

$$\text{Dittus-Boelter equation}: \quad Nu = 0.023 Re^{0.8} Pr^{n} \tag{3}$$

$$\text{Blasius equation}: \quad f = 0.079 Re^{-1/4} \tag{4}$$

where n is 0.4 for heating and 0.3 for cooling of fluid.

The heat transfer ratio (Nu/Nu_p) and friction factor ratio (f/f_p) of 70 tubes which yield the best thermal performance among those studied are summarized in Table 2. The ratio in the table is experimental values for different enhanced tubes over plain tube from the same literature. Reynolds number in the study was normally in the range of $1–100 \times 10^3$, mostly in the transition region and turbulent flow. Working fluids for internally finned tubes are all air.

For gases, rib height has important effects on Nu/Nu_p. Typically, the tubes with small fin height yield small heat transfer enhanced ratio, while the friction factor ratio is less than tubes with high fin. Prandtl, Reynolds and Biot numbers should be important dimensionless numbers for fin efficiency evaluation. The fin number per circle for gases is less than liquids, which is typically less than 15 according to the review. It is normally within 45 for liquid enhancement with internal fins [6,23–27]. The helix angle for most of internal fins with gas is 0° or 90°.The heat transfer enhancement with fins was usually accomplished with an considerable increase in pressure drop such as [28]. The possible enhancement mechanism associated with high performance of tubes is fin induced turbulence and area increase. The rib height, helix angle and number of starts have important effects on heat transfer augmentation. High fin, 0° or 90° helix angle and less starts number are the major features for gas heat transfer augmentation. As the increase of fin height, heat transfer rate is increasing. However, a rather modest increases might be observed when the height reaches a critical value.

The best heat transfer performance was given by the tube in [28]. The heat transfer enhancement was obtained with internal wave-like longitudinal fins. The center of tube was fully blocked and no flow went through. The significant heat transfer enhancement obtained from the two tubes might be attributed to: (1) Total heat transfer surface area of blocked tube was 7.1 times over smooth one. (2) The center of tube was fully blocked, the flow rate in annulus increases and hence heat transfer in annular space was enhanced. It should be noted that there was also an accompanying large increase in friction factor. Similar tube in [30] also provided a higher improvement in average heat transfer coefficient.

The fins with complex structures might cause a higher pressure drop. It is partially due to larger contacting areas between gas and wall. The fins like wave [28,30,31] and T-section fins [32] may

Table 1
Correlations for internally finned tubes of gas pipe flow.

Investigators	Tube geometry/Fluid	Validation range	Friction factor	Heat transfer
Smithberg and Landis [29]	Twisted-tape inserts	$0.7 \le Pr \le 10$	$f = \left[0.046 + 2.1\left(\frac{H}{d_i} - 0.5\right)^{-1.2}\right] Re^{-n}$	$Nu = \frac{(1+2\eta_e/\pi)RePr}{1+\frac{700}{Ref}\left(\frac{d_i}{H}\right)\left(\frac{d_h}{d_i}\right)Pr^{0.731}}$ $\left[\frac{50.9(d_i/H)}{Re\sqrt{f}} + 0.023\left(\frac{d_i}{d_h}\right)Re^{-0.2}Pr^{-2/3}\left(1+\frac{0.0219}{\left(\frac{H}{d_i}\right)^2 f}\right)\right]^{1/2}$
	Twist ratio: y:3.62–22	$2000 \le Re \le 10^5$	$n = 0.2\left[1 + 1.7\left(\frac{H}{d_i}\right)^{-1/2}\right]$	$\eta_e = \frac{\eta_f}{1+\eta_f\frac{Ehd_i}{\dot{c}_f A}}$. $\eta_f = \frac{Q}{hA_{fin}(T_w - T_f)}$
	Air, water Units used in this paper is: ft, Btu, hr, F	Accuracy: f: ±10% Nu: ±20%		A_{fin} wetted surface area
Webb et al. [5]	Repeated transverse ribs: $0.01 \le e/d_i \le 0.04$ $10 \le p/e \le 40$ Air, water, n-butyl alcohol	e^+>35 $6000 \le Re \le 100000$ $0.71 \le Pr \le 37.6$ Accuracy: ±11%	$f = 2[2.5ln(d_i/2e) + 0.95(p/e)^{0.53} - 3.75]^{-2}$ $e^+ = (e/d_i)Re\sqrt{f/2}$	$Nu = \frac{(f/2)RePr}{1+\sqrt{f/2}[4.5(e^+)^{0.28}Pr^{0.57} - 0.95(p/e)^{0.53}]}$
Han[16]	Repeated transverse ribs $5 \le p/e \le 20$, $0.032 \le e/d_h \le 0.102$, β: 20°–90° e/w: 0.67–1 Air	$7.5 \times 10^4 \le Re \le 2 \times 10^5$ Pr = 0.7 Accuracy: within ±40%	$f = 2(Re^+ - 2.5ln(2e/d_h) - 3.75)^{-2}$ $Re^+ = 4.9(e^+/35)^m/[(\alpha/90°)^{0.35}(10/P/e)^n \times (\beta/45)^{0.57}]$ If $e^+ < 35$, $m = -0.4$; If $e^+ \geqslant 35$, $m = 0$; If $P/e < 10$, $n = -0.13$; If $P/e \geqslant 10$, $n = 0.53(\beta/90°)^{0.71}$	$Nu = \frac{fRePr}{[He^+ - Re^+](2f)^{1/2}+2}$ $He^+ = 10(e^+/35)^i/(\alpha/45°)^j$ $i = 0$, when $e^+ < 35$; $i = 0.28$, when $e^+ \geqslant 35$; $j = 0.5$, when $\beta < 45°$; $j = -0.45$, when $\beta \geqslant 45°$;
Carnavos [20]	Helical and longitudinal ribs. d_i: 8–22.2 mm, N_s: 6–38 e: 0.6–2 mm, α: 0–30°, δt: 0.26–0.8 mm. Air, water, and ethylene glycol-water	$1 \times 10^4 \le Re \le 10^5$ $0.7 \le Pr \le 30$ Accuracy: within ±10%	$f = 0.046Re^{-0.2}(F^*)^{-1}$ $F = (A_{fa}/A_{fn})^{0.5}(\sec\alpha)^{0.75}$	$Nu = 0.023Re^{0.8}Pr^{0.4}(F)$ $F = (A_{fa}/A_{fc})^{0.1}(A_n/A_a)^{0.5}(\sec\alpha)^3$
Kader and Yaglom [17]	Repeated transverse ribs e^+: 10–4000 $4 \le p/e \le 40$,	$3 \times 10^4 \le Re \le 2 \times 10^5$ $0.7 \le Pr \le 4585$ Agree satisfactorily with experiment result	$f = \frac{\Delta P d_i}{2L\rho v^2}$	$Nu = \frac{1.42(f/2)^{0.5}RePr}{5(e^+)^{0.25} - 3\ln(e/d_i) + 5.6 - 4.5/(1-e/d_i)^2 + 9.5(f/2)^{0.5}}$
Gee and Webb[18]	Transverse and helical ribs α: 30°, 49°, 70°, p/e = 15 Air	$6 \times 10^3 \le Re \le 6.5 \times 10^4$ Pr = 0.71 Compared with literature	$f = 2[\overline{B}(e^+,\alpha)/(\alpha/50)^{0.16} - 2.5\ln(2e/d_i) - 3.75]^{-2}$ $\overline{B}(e^+,\alpha)$: Friction similarity function	$Nu = \frac{(f/2)^{0.5}RePr}{1+\sqrt{f/2}[\overline{g}(e^+,Pr,\alpha)/(\alpha/50)^j - \overline{B}(e^+,\alpha)]}$ $j = 0.37$ for $\alpha < 50°$; $j = -0.16$ for $\alpha > 50°$ $\overline{g}(e^+,Pr,\alpha)$: Heat transfer similarity function
Kim and Webb[19]	Experimental result from Carnavos [22] Air, water, and ethylene glycol-water	$1 \times 10^4 \le Re \le 10^5$ $0.7 \le Pr \le 30$ Accuracy: f: ±10% Nu: ±15%	$f = 2\left[\frac{2N_s}{\left(b+\frac{p_i-t_t}{2}\right)}[b(A' + 2.5\ln(e) - 3.75) + \frac{p_i-t_t}{2}(A' + 2.5\ln(\frac{p_i-t_t}{2}) - 3.75)]\cdot(A_f/A) + \left[\frac{1}{(1-2e/d_i)^2}2.5\ln\left(\frac{d}{d_h}Re\sqrt{f/2}\right) - \frac{4e/d_i-(2e/d_i)^2}{1-(2e/d_i)^2}2.5\ln\left(\frac{e}{d_h}Re\sqrt{f/2}\right) - 2.5\frac{1.5-4e/d_i+2(e/d_i)^2}{(1-(2e/d_i))^2} + 5.5\right]\cdot(A_c/A)\right]^{-2}$	$Nu = RePr\left\{\frac{2N_s}{(b+(p_i-t_t)/2)}[b(A'C' + (2.5A' + A_sC')(\ln(e) - 1.5) + 2.5A_s(\ln(e)(\ln(e) - 3) + 3.5)) + (p_i - t_t)/2(A'C' + (2.5A' + A_sC')\cdot(\ln((p_i - t_t)/2) - 1.5) + 2.5A_s(\ln((p_i - t_t)/2)(\ln((p_i - t_t)/2) - 3) + 3.5))]\cdot(A_f/A) + [A'C'(1 - 2e/d_i) + 2.5(A' + C')(\ln(d_i/2) - (2e/d_i)\ln(e) - 1 + 2e/d_i) + 6.25(\ln^2(d_i/2)$

(*continued on next page*)

Table 1 (*continued*)

Investigators	Tube geometry/Fluid	Validation range	Friction factor	Heat transfer
			$A' = 2.5\ln(Re\sqrt{f/2}/d_h) + 5.5$ $C' = A_s\ln(Re\sqrt{f/2}/d_h) + B_s$	$-(2e/d_i)\ln^2(d_i/2) - 2\ln(d_i/2) + (2e/d_i)\ln(e)$ $+2 - 2(2e/d_i)) - 0.5A'C'(1 - (2e/d_i)^2)$ $-1.25(A' + C')(\ln(d_i/2) - (2e/d_i)^2\ln(e)$ $-0.5 - 0.5(2e/d_i)^2) - 1.563[2(\ln^2(d_i/2) - \ln(d_i/2))$ $-2e^2(\ln^2(e) - \ln(e)) + 1 - (2e/d_i)^2]\cdot(A_c/A)\}]^{-1}$ $B_s = 5\ln(\frac{5Pr+1}{30}) + 8.55 + 5Pr$
Ravigururajan and Bergles [21]	e/d_i : 0.01 – 0.1 p/d_i : 0.1 – 1.0 $\alpha/90$: 0 – 1.0	10,000 < Re < 100,000 $0.7 \le Pr \le 35$ Accuracy: f: 77% of data(1658 points) within ±20% Nu: 69% of data (18,070 points) within ±20%	$f/f_p = 0.25\times\left\{1 + \left[29.1Re^{(0.67-0.06p/d-0.49\alpha/90)}\right.\right.$ $\times(e/d)^{(1.37-0.157p/d)}\times(p/d)^{(-1.66Re\times10^{-6}-0.15p/d)}$ $\left.\left.\times(1 + 2.94\sin(45/Ns))\right]^{15/16}\right\}^{16/15}$	$Nu/Nu_p = \left\{1 + \left[2.64Re^{0.036}(e/d)^{0.212}\times(p/d)^{-0.21}\right.\right.$ $\left.\left.\times(\alpha/90)^{0.29}(Pr)^{0.024}\right]^7\right\}^{1/7}$
Layek et al. [22]	$0.022 \le e/d_h \le 0.04$ $4.5 \le p/e \le 10$ $0.3 \le g/p \le 0.6$ $0° \le \phi \le 30°$	3000 < Re < 21,000 Pr = 0.7 Accuracy: Nu: 93% (456 out of 488) within 2.8% f: 93%(455 out of 488) within ±15%	$f = 0.00245Re^{-0.124}(e/d_h)^{0.365}(p/e)^{4.32}\cdot$ $(g/p)^{-1.124}\exp[0.005\phi]\cdot\{\exp[-1.09(\ln(p/e^2))]\}\cdot$ $\{\exp[-0.68(\ln(g/p)^2)]\}$	$Nu = 0.00225Re^{0.92}(e/d_h)^{0.52}(p/e)^{1.72}(g/p)^{-1.21}\cdot$ $\phi^{1.24}\{\exp[-0.22(\ln\phi)^2]\}\{\exp[-0.46(\ln(p/e^2))]\}$ $\{\exp[-0.74(\ln(g/p)^2)]\}$

cause greater pressure drops. The pressure drop penalties are less for simple and thin fins. The pressure drop for high fin tubes is higher than micro-fin tubes for gas except that with inserts [6].

Fig. 3 shows the Nu/Pr^n for internally finned tubes published since 1971 for gases with more than 109 experimental measurements. Nu/Pr^n and Reynolds number are displayed on the ordinate and abscissa, respectively. The index n is 0.4 for heating and 0.3 for cooling or indicated by the author of paper. Most of the investigations on pipe flow heat transfer enhancement techniques of gases are conducted on air for heating. Thus, Air and $Nu/Pr^{0.4}$ are omitted in the figure captions and other circumstances are indicated individually. Reynolds number ranged from 2000 to 120,000. Dittus-Boelter equation ($0.023\times Re^{0.8}$) for plain tube is also presented in Fig. 3 for reference. The lines designated by 1×, 2×, 4× and 6× show the augmentation ratio over the value predicted by Dittus-Boelter equation. As shown in the figure, enhanced ratios of most tubes are in the range of 1–4. The Nu/Pr^n exhibits an almost linear trend with Reynolds number, and the slopes are very close to D-B equation.

Fanning friction factors are shown in Fig. 4. For ease of reference, the curves 1×, 2×, 4× and 13× are devised to designate the increase ratios over the value predicted by Blasius equation ($0.079Re^{-1/4}$). As indicated in Fig. 4, the ratios of friction factor for most internally finned tubes are from 1 to 8 compared with plain tube, which are generally larger than that of heat transfer enhancement ratios. While, for liquid, the heat transfer enhancement and friction factor ratios are typically very similar [40–42]. Among all the internally finned tubes, friction factors of three tube with wave like fin [28,30,31], T-section fins [32] and transverse ribs [5] are at the highest level. The friction factor of transverse ribs in [5] increased by as much as a factor of 13. However, as can be seen in Fig. 3, only up to 250% increase of internal heat transfer coefficient was obtained.

2.4. Thermal-hydraulic performance evaluation of internally finned tubes

The performance evaluation plot proposed by Fan et al. [7] is adopted to assess the thermal-hydraulic performance of aforementioned enhanced tubes. In the evaluation, the reference values of heat transfer and friction factor for plain tube are determined by Dittus-Boelter and Blasius equation, respectively. The ratio of friction factor of enhanced tube over plain tube and the ratio of heat transfer augmentation at the same Reynolds number are taken as the abscissa and ordinate, respectively. By using performance evaluation plot, heat transfer and flow friction can both be precisely considered. It should be noted that the evaluation for enhanced tube in this study is based on the same inner diameter (d_i). For internally finned tube, inner diameter is to the root of internal fins.

In Fig. 5, experimental data for internally finned tubes in Figs. 3 and 4 are presented in the performance evaluation plot. Energy saving effectiveness of different enhanced internal fins can be clearly illustrated based on the same reference. Region 1 is characterized by heat transfer enhancement without energy-saving. The enhancement of heat transfer rate is less than the increase of power consumption. In Region 2, heat transfer can be enhanced with same pump power consumption, where heat transfer improvements is higher than reference tube under the same pumping power consumption. In Region 3 heat transfer is enhanced per identical pressure drop, where heat transfer augmentation is higher than reference tube under the same pressure drop. Region 4 is the most favorable occasion, where heat transfer enhancement is more than the increase of friction coefficient obtained under the same flow rate. It is important to note that at the same ratio of f_f/f_r, the more the heat transfer being augmented, the more difficult to accomplish.

Table 2
Experimental studies on gas in internally finned tubes.

Investigators	*Re*	Fluid	Tube/number	Best tube/Features	f/f_p	Nu/Nu_p
Webb et al. [5]	$6–100 \times 10^3$	Air	Low-fin/5	$e/d_i = 0.04$, $d_i = 38.6$, $p/e = 10$, $\alpha = 90°$	6.8–14.4	2.4–2.8
Carnavos [33]	$10–100 \times 10^3$	Air	Low-fin/21	$e/d_i = 0.084$, $d_i = 23.8$, $N_s = 16$, $\alpha = 20°$	1.6–1.9	1.7–1.9
Gee and Webb [18]	$6–65 \times 10^3$	Air	Low-fin/3	$e/d_i = 0.01$, $d_i = 25.4$, $p/e = 15$, $\alpha = 70°$	1.5–2.1	1.4–1.6
Han [34]	$7–90 \times 10^3$	Air	High-fin (square ducts)/5	$e/d_i = 0.21$, $d_h = 70$, $p/e = 6$, $\alpha = 90°$	4.3–6.5	1.9–2.5
Huq et al. [35]	$26–78 \times 10^3$	Air	High-fin/1	$e/d_i = 0.21$, $d_i = 70$, $N_s = 6$, $\alpha = 0°$	3.2–4.5	2.0–2.1
Uddin [36]	$18–40 \times 10^3$	Air	High-fin/1	$e/d_i = 0.21$, $d_i = 70$, $N_s = 8$, $\alpha = 0°$	5.9–7.2	1.5–1.8
Yu et al. [28]	$0.9–3.5 \times 10^3$	Air	Wave-like fin/2	$d_i = 33$, 20 waves	10.8–13.6	4.8–7.1
Tao et al. [37]	$5–50 \times 10^3$	Air	High-fin/5	$e/d_i = 0.375$, $Ns = 9$, $p/e = 2.81$, $\alpha = 0°$	3.6–3.8	2.7–3.5
Yu and Tao [30]	$2–15 \times 10^3$	Air	High-fin/5	$e/d_i = 0.375$, $Ns = 9$, $p/e = 2.81$, $\alpha = 0°$	6.5–7.6	3.6–3.9
Layek et al. [22]	$3–21 \times 10^3$	Air	Low-fin/6	$e/d_i = 0.03$, $p/e = 6$	2.7–4.2	2.3–3.0
Islam and Mozumder [32]	$20–50 \times 10^3$	Air	T-section fins/1	$e/d_i = 0.257$, $Ns = 6$, $\alpha = 0°$	2.0–14.9	2.2–2.8
El-Sayed et al. [38]	$3–40 \times 10^3$	Air	High-fin/5	$e/d_i = 0.25$, $Ns = 6$, $\alpha = 0°$	1.9–2.0	1.7–2.1
Dipti and Kailash [39]	$7–12 \times 10^3$	Air	High-fin/1	$e/d_i = 0.227$, $Ns = 4$, $\alpha = 0°$	2.1–2.5	3.3–3.5
Peng et al. [31]	$2–20 \times 10^3$	Air	High-fin/9	$e/d_i = 0.284$, $Ns = 6$, $\alpha = 0°$	5.7–10.6	1.4–2.0

As shown in Fig. 5, the data for internally finned tubes mainly located in Regions 3, only a portion of points for the tube in [31,36] located in Regions 2 and very few data located in Region 4. For most tubes, the increment of friction factor is higher than increment of heat transfer rate at the same flow rate. It is interesting to note that the heat transfer enhanced ratios, are almost invariable or decrease with increment of friction factor ratio for all the tubes presented in Fig. 5. For example, friction factor ratio of the tube in [5] increased from 7.2 to 13.7, while the heat transfer enhanced ratio generally maintains 2.5. It implies that the performance of a specific geometry might have its limit in heat transfer and further upgrading is difficult. In other words, increasing of gas velocity has minor effect on heat transfer enhancement ratio while lead to higher pressure drop. The tubes located in Region 4 have higher effectiveness of saving energy.

3. Tubes with twisted tapes, coils and turbulence promoters inserts

3.1. Introduction of tube with inserts

The enhancement techniques can also be various devices inserted in a smooth circular tube. Different types of inserts are shown in Fig. 6. Inserts can stimulate turbulence, promote transverse mixing, and hence enhance the forced convection heat trans-

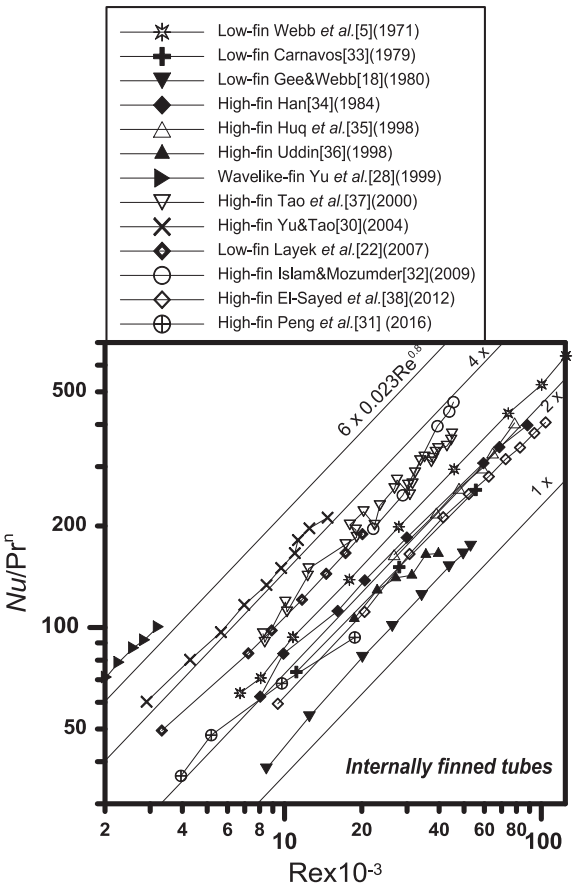

Fig. 3. Nu/Pr^n versus *Re* for internally finned tubes.

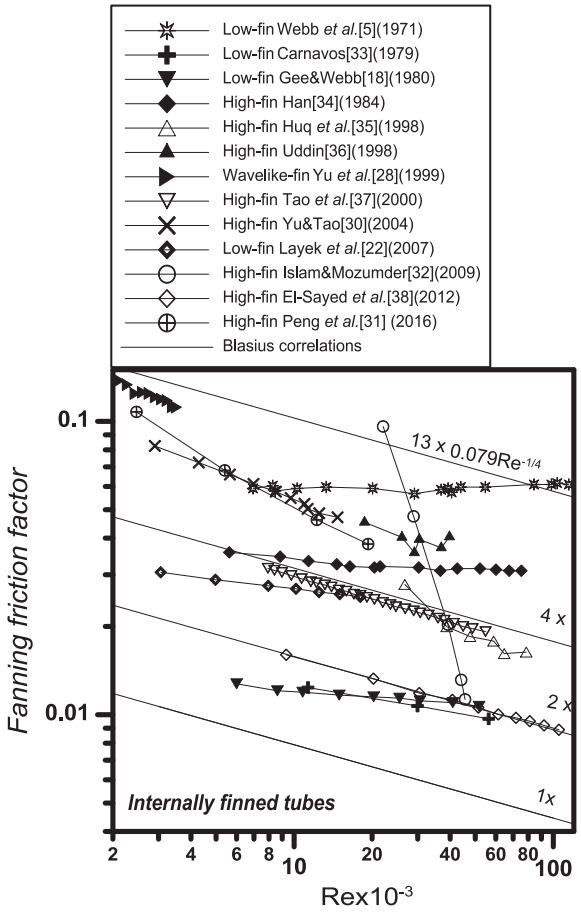

Fig. 4. Fanning friction factor versus *Re* for internally finned tubes.

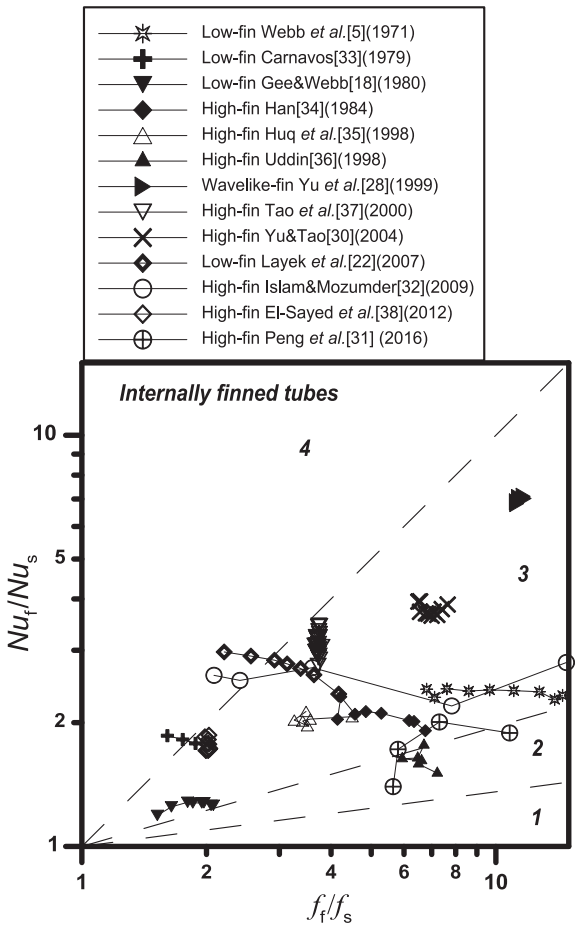

Fig. 5. Performance evaluation plot for internally finned tubes from literature.

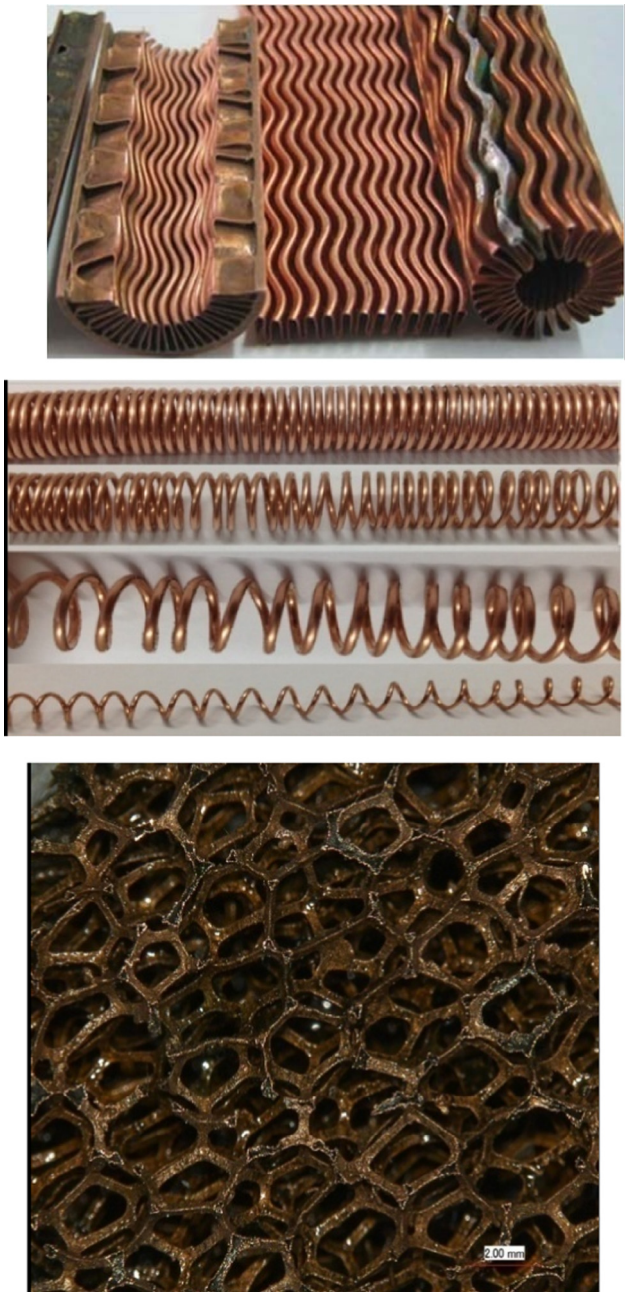

Fig. 6. Different types of inserts.

fer. Frequently used inserts include tapes [43], wire coils, rings [44], strips, static mixing elements [45,46], swirl flow generators or porous media [47]. Through different types of inserts, turbulence intensity can be increased significantly under different flow regimes. Reynolds number (Re), Prandtl number (Pr) are the two major controlling factors affecting the friction and heat transfer. The geometric parameters of inserted twisted tapes (Fig. 7) also include: 180° twist pitch, H; tape width, w; tape thickness, δ; and internal diameter of tube, d_i. Twist ratio is $y = H/w$. The twist ratio can be $y = \infty$, which is a straight tape insert dividing the flow into two semicircular segments. Due to larger contacting areas, the friction factor is usually increasing as the reduction of twist ratio. According to the survey, there are relatively few correlations (for heat transfer coefficient and friction factor) available for laminar and turbulent gas flow, for both inserted tapes and swirl generators [29,48–51]. The general correlations are not yet available and the accuracy may not be guaranteed.

3.2. Experimental data

Experimental data on the heat transfer and friction factor of tubes fitted with twisted tape, coil, and swirl generator are summarized in Table 3. Systematic survey indicates that the number of papers on the tube with different forms of inserts is more than internally finned tubes. Reynolds number in the investigations are within 120×10^3. Twist ratio (y) is normally in the range of 0.4–4.72. It is found that the heat transfer augmentation ratios are higher in the laminar and transitional region. It is consistent with the survey of liquids. The pipes involved in Table 3 is totally

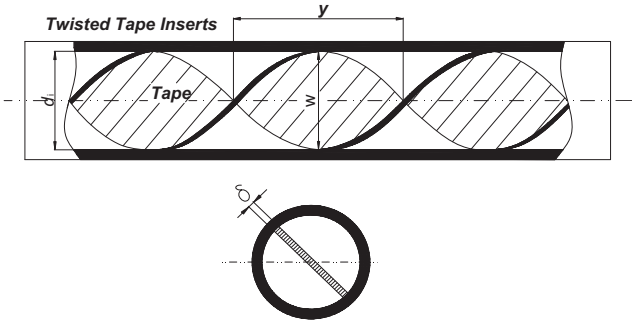

Fig. 7. Schematic diagram of pipes with twisted tape inserts.

Table 3
Experimental data for tubes with twisted tape and other inserts.

Investigators	*Re*	Fluid	Tube/number	Best tube/Feature	f/f_p	Nu/Nu_p
Smithberg and Landis [29]	$20–50 \times 10^3$	Air	Twisted tape/5	$y = 3.62$	2.2–2.4	2.8–3.1
Yilmaz et al. [61]	$20–120 \times 10^3$	Air	Vane swirl generator/5	Vane angle 75°	18.7–20.1	1.8–2.2
Wang and Sunden [62]	100–600	Air	Twisted-tape and coil/9	$y = 0.42$	45.4–46.7	2.0–6.7
	$5–45 \times 10^3$				22.8–23.6	3.3–3.4
Yilmaz et al. [63]	$20–120 \times 10^3$	Air	Vane swirl generator/15	No deflecting	10.3–16.9	1.7–2.7
Eiamsa-ard et al. [64]	$2.3–8.8 \times 10^3$	Air	Twisted tape /1	Full-length helical/rod	8.0–18.7	1.3–1.5
Yakut and Sahin [65]	$6–38 \times 10^3$	Air	Coiled wire/3	$y = 0.6$	18.8–22.3	1.9–3.5
Yakut and Sahin [52]	$6–15 \times 10^3$	Air	Conical-rings/3	$y = 0.2$	174–196	3.5–5.3
Eiamsa-ard and Promvonge [66]	$2.3–8.8 \times 10^3$	Air	Twisted tape /10	Full-length helical/rod	7.8–9.1	1.3–1.5
Eiamsa-ard and Promvonge [53]	$2.4–15.8 \times 10^3$	Air	V-nozzle inserts /3	$p/d_i = 2.0$	42.3–51.5	2.5–7.3
Promvonge and Eiamsa-ard [67]	$8.5–16.6 \times 10^3$	Air	Nozzle inserts/9	D-nozzle, $p/d_i = 2.0$	157–219	3.2–3.4
Promvonge and Eiamsa-ard [68]	$8.5–16.6 \times 10^3$	Air	Nozzle inserts/6	D-nozzle, $p/d_i = 2.0$	108–111	2.6–2.9
Chang et al. [50]	$1–40 \times 10^3$	Air	Broken twisted tape/6	$y = 1$	14.9–24	2.5–3.4
Meng et al. [69]	$4–20 \times 10^3$	Air	Twisted tape/4	$y = 4.72$	5.0–6.3	1.3–2.3
Promvonge and Eiamsa-ard [54]	$6–26 \times 10^3$	Air	Conical-ring combined with twisted tape insert/3	$y = 3.75$	158–169	3.0–5.9
Promvonge [70]	$5–25 \times 10^3$	Air	Coiled square wires/4	$p/d_i = 0.32$	9.6–10.1	2.2–2.7
Promvonge [71]	$3–16 \times 10^3$	Air	Wire coils combined with twisted tapes/8	$p/d_i = 4$; $y = 4$	53–71	3.6–6.6
Eiamsa-ard et al. [72]	$5–18 \times 10^3$	Air	Dual twisted tape/5	$y/w = 3$	2.6–3.9	1.4–1.5
Eiamsa-ard et al. [73]	$4–20 \times 10^3$	Air	Swirl generator/6	PR = 5, blade angle = 60° and N = 8.	8.1–11.7	2.0–2.2
Kurtbaş et al. [74]	$10–35 \times 10^3$	Air	Swirl generators/6	DR = 0.166 swirl generator angle = 30°	15–55	3.1–5.1
Chompookham et al. [75]	$5–23 \times 10^3$	Air	Combined wedge rib and winglet /9	Wedge and winglet angle 60°	31–45	3.4–3.8
Gunes et al. [76]	$3.5–27 \times 10^3$	Air	Coiled wire inserts/5	$a/d_i = 0.089$, $p/d_i = 1$	6.0–6.5	2.1–2.5
Depaiwa et al. [77]	$5–23 \times 10^3$	Air	Swirl generators/6	PD, swirl generator angle = 60°	4.3–6.2	1.8–1.9
Eiamsa-ard and Promvonge [78]	$4–20 \times 10^3$	Air	Serrated twisted tape/4	Serration depth/tape width = 0.3	3.8–4.7	1.4–1.7
Eiamsa-ard et al. [79]	$5–20 \times 10^3$	Air	Wire coils combined with twisted tapes/11	DI-coil, $y = 3$	32.6–33.1	2.6–3.1
Kongkaitpaiboon et al. [55]	$4–20 \times 10^3$	Air	Perforated conical-rings/15	CR, Pitch ratio = 4	128–164	3.3–4.2
Eiamsa-ard and Promvonge [80]	$4–16 \times 10^3$	Air	Swirl generator /9	Tail length ratio = 0.3	7.6–8.0	1.3–1.6
Ahamed et al. [81]	$13–52 \times 10^3$	Air	Perforated twisted tape /7	$y = 4.55$, 4.6% perforation	1.4–2.7	1.9–2.5
Bhuiya et al. [56]	$20–50 \times 10^3$	Air	Twisted tapes/4	Helical angle = 9°	2.2–3.0	3.3–3.9
Eiamsa-ard et al. [82]	$6–20 \times 10^3$	Air	Twisted tapes/12	$p/d_i = 1$, Helically twisted	47.0–50.5	2.0–2.3
Bas and Ozceyhan [60]	$5.1–25 \times 10^3$	Air	Twisted tapes/10	$y = 2.0$	3.1–4.1	1.9–2.6
Bhuiya et al. [57]	$7–50 \times 10^3$	Air	Perforated twisted tapes/4	Porosity = 4.5%, $y = 1.92$	2.4–4.6	2.5–3.9
Bhuiya et al. [58]	$7–50 \times 10^3$	Air	Triple twisted tapes/4	$y = 1.92$	2.3–3.9	2.3–3.4
Bhuiya et al. [59]	$7–50 \times 10^3$	Air	Double twisted tapes/4	$y = 1.95$	2.3–3.6	2.1–3.1
Bhuiya et al. [43]	$7–50 \times 10^3$	Air	Perforated double counter twisted tapes/4	Porosity = 4.6%, $y = 1.92$	2.4–4.0	2.3–3.5

226. Similarly, heat transfer ratio (Nu/Nu_p) and friction factor ratio (f/f_p) of the pipe which gives the best heat transfer performance are summarized.

The friction factor increased ratio for swirl generator is mostly very high. As can be seen in Table 3, the pressure drops increased as much as 160 times higher in [52–55], while the heat transfer enhanced ratio is typically within 10. Normally, the swirl generators such as conical-rings, V-nozzle inserts, and compound enhancement techniques like combined wedge rib and winglet, wire coils combined with twisted tapes have a higher pressure drop than twisted tapes acting alone.

For enhancement techniques with only simple twisted tapes or coils, the friction factor and heat transfer increment are regularly moderate. In most cases, heat transfer augmentation ratio for gases are in the range of 2–4 and friction factor increment ratio are higher than heat transfer. While, increase of friction factor in [29,43,56,57] is lower than increase of heat transfer. It is quite beneficial for heat exchanger design. It is also found that twisted tapes with perforated holes might have lower pressure drop [43,57]. The pressure drop of double, triple twisted tapes have insignificant effects on friction factor. With similar twisted ratios, the pressure drop and heat transfer increase with triple inserts were only a little bit higher than double inserts [58,59].

Because twisted tape inserts can be either tight or loose, the effect of geometry parameters on the heat transfer and friction factor cannot be easily identified and interpreted quantitatively. Experimental results indicated that the twist ratio was the major affecting factor. Combined the effects of perforated holes, serrations, notches, it makes the heat transfer prediction even more difficult. Typically, with the twisted tape acting alone and $y = 2$, the friction factor increase is moderate and around 2.4–4 according to the investigations [43,56–60].

The experimental data reported in literature listed in Table 3 are also presented in Figs. 8 and 9. Fig. 8 shows the Nu/Pr^n against Reynolds number for 33 tubes fitted with twisted tapes or other turbulence promoters. Fig. 9 shows the Fanning friction factor versus Reynolds number. Dittus-Boelter and Blasius equation for plain tube are also presented in the figures. Similarly, in order to confirm the comparison is based on the same reference, experiment data for plain tube reported in the literature is also compared with Dittus-Boelter and Blasius equation. They are found to be in good agreement with the two equations. The disagreements of Nusselt number and friction factor for the 33 papers were mostly within 20%.

As shown in Fig. 8, the slopes Nu/Pr^n versus Reynolds number for different twisted tape inserted tubes are very similar and gathering in a narrow zone. The heat transfer enhanced ratios are regularly in the range of 1.5–6.0, which is consistent with that of liquids [6]. The heat transfer enhanced ratio increased for some tubes as the Reynolds number are lower than 10×10^3. These tubes are all fitted with swirl promoter or combined with two or more enhancement techniques. It indicated that some swirl promoters have additional enhancement effect in the transitional region. For most of other tubes, heat transfer enhanced ratio is nor-

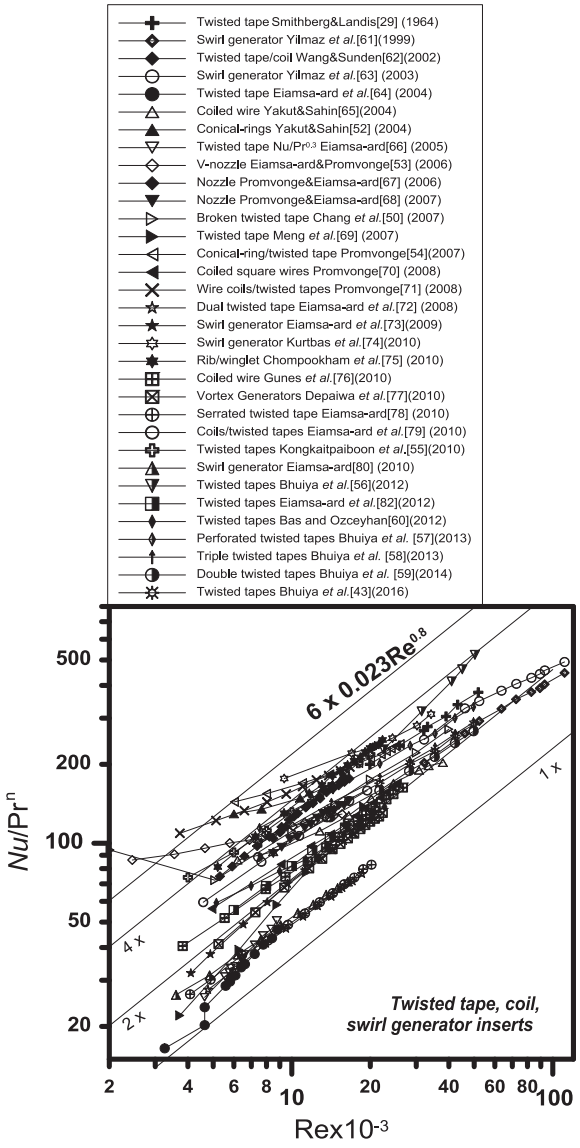

Fig. 8. Nu/Pr^n versus *Re* for tubes fitted with twisted tape inserts and swirl promoters.

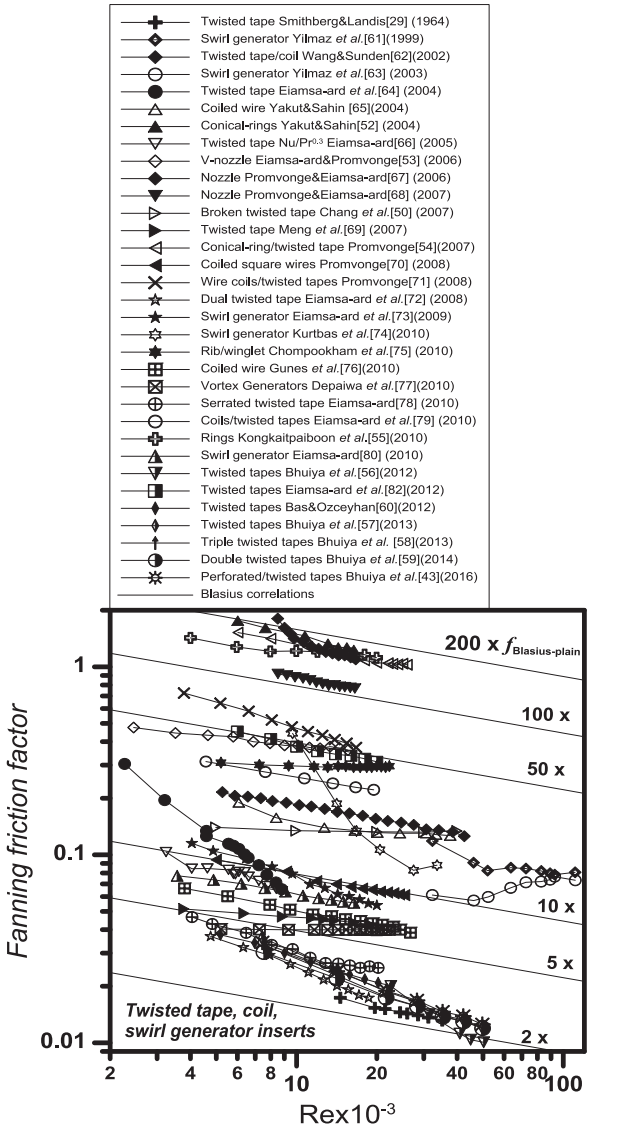

Fig. 9. Fanning friction factor versus *Re* for tubes fitted with twisted tape inserts and swirl promoters.

mally maintained at a certain level in Reynolds number of 3×10^3 to 100×10^3.

In Fig. 9, the friction factors ratios for 17 tubes are within 10 and other 16 tubes are in the range of 10–200. The ratios within 10 are mostly with twisted tape inserts acting alone and twisted ratios are moderate. The tubes with friction factor enhanced ratio greater than 10 are mostly turbulence promoters except some compound enhancement techniques, which are wire coils combined with twisted tapes [71,79], helically twisted tapes [82], or rib and vortex generators [75]. The friction factor ratios are in the range of 10 to 50 times or higher. The inserts in [52,54,67,68] give the largest increase of friction factor. These tubes are all fitted with turbulence-promoter, such as conical nozzle or rings.

3.3. Thermal-hydraulic performance evaluation of tubes with tape and other inserts

In order to assess the comprehensive thermal-hydraulic performance of the tube fitted with twisted tapes, coils and swirl generators, the experimental data in Figs. 8 and 9 totally 33 tubes are all presented in the performance evaluation plot (see Fig. 10). The plot enables the comparison of all the data with the same reference at a given Reynolds number. For the tubes fitted with twisted tapes or coils and swirl generators, nearly all the data falls into the Regions of 2 and 3 in the Reynolds number 2×10^3 to 200×10^3. As shown in Fig. 10, for tubes with different kinds of inserts, the heat transfer enhanced ratio is within 6, and the friction factor increased ratio is evenly distributed in the region of 2–200. Therefore, the data mostly located in the lower region of evaluation plot, which means the heat transfer enhancement is moderate while the friction factor increment is higher.

The tubes in [43,57–59,66] located in the boundary of Region 4 and 3, which have a higher comprehensive thermo-hydraulic performance. For the tubes in [29,56], heat transfer enhancement is higher than increase of pressure drop, which is the most beneficial. The tubes located in Region 4 and in the boundary of Region 4 and Region 3 are all twisted tapes acting alone. The tubes [64] located in Region 1 is featured by improved heat transfer without energy-saving. As indicated above, the swirl promoters have a relatively higher pressure drop and the data mostly located in the region approaching Region 2. Generally, the thermal-hydraulic perfor-

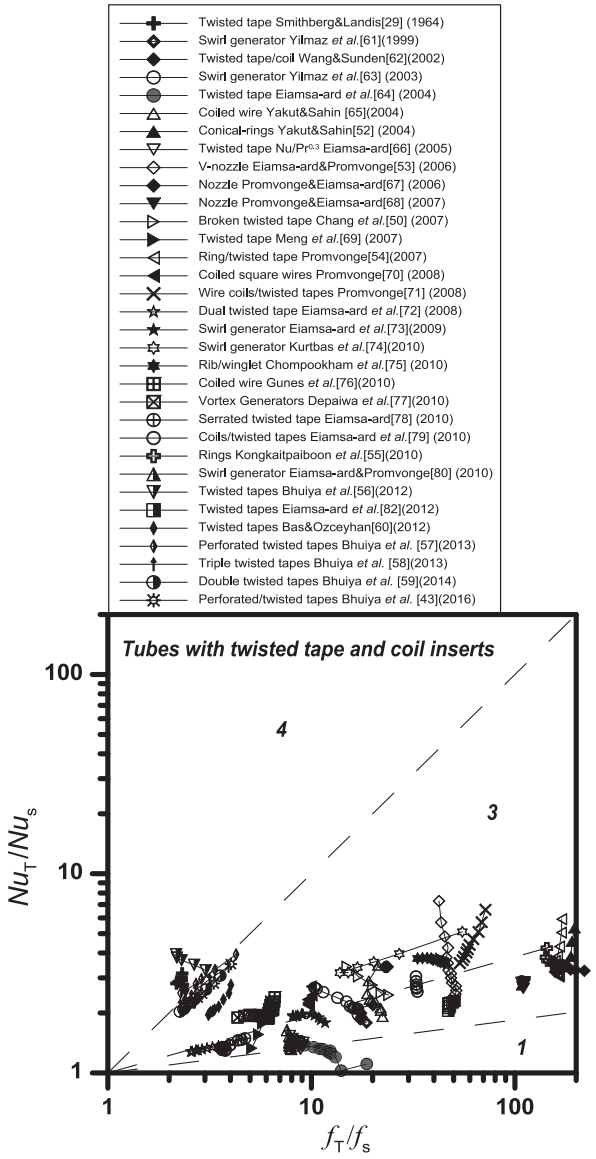

Fig. 10. Performance evaluation plot for tubes fitted with twisted tape inserts and swirl promoters.

mance of twisted tape inserts are better than tubes fitted with swirl generators.

4. Corrugated tubes

4.1. Introduction of corrugated tubes

The twisted tube, tube with corrugations, spirally fluted tubes, convoluted, wavy, indented and other deformation made on the basic tubes all belong to the group of corrugated tubes. The picture of corrugated tube are shown in Fig. 11. The corrugations might have single or multi starts. Because the heat transfer area is increased and mixing of fluids is promoted with deep corrugations, they are also used to enhance the convective heat transfer of gases. When turbulent flow in the central region is disturbed by spiral indentations, the boundary layer thickness is reduced by flow colliding against the indentations and hence eddy current occurs. It has been demonstrated that the deformations made on the tube can produce a substantial heat transfer enhancement. The geometry parameters (Fig. 12) include pitch (p), indent width (w) and

Fig. 11. Corrugated tubes.

maximum height (e) of indent, and number of starts (N_s) for multi-starts deformation.

According to the survey, corrugated tubes were mainly adopted to enhance the heat transfer of liquids [6]. Only a relatively small number of investigations are carried out on gases. The pressure drop should be less than twisted tape or swirl promoter. The advantage of corrugated tube is lower fouling potential when used in exhaust flue gas heat recovery. It is quite useful for heat recovery compared with inserted tapes or fins. While, if very hot gases flow through the tube side, fouling caused by small particles or chemical reaction has an unfavorable effect on the heat transfer, which diminishes the performance.

4.2. Experimental measurements

Typical experimental data and some numerical investigations for the heat transfer performance and friction factor of gases inside corrugated tubes are summarized in Table 4. The best performed tube is presented in the table for the investigation involving more than one tube. Basic geometry parameters of the tube are also provided. p/d_i for the tube ranges from 0.1 to 2.94 and e/d_i is from 0.02 to 0.25. The test fluid include air, N_2, He, and exhaust gases. The Reynolds number is in the region of 5–260 $\times$ 10^3.

The largest Nu/Nu_p is 3.0 for corrugated tube and the average ratio is in the range of 1.5–3. Most of heat transfer enhanced ratio is mainly in the range of 1–2 without the combined effect of any other enhancement techniques. The pressure drop increases are in the range of 2–10. The corrugated tubes with swirl generator inserts had a higher pressure drop. However, the contributions to heat transfer is rather mild. Normally, the overall heat transfer coefficient increases when p/d_i decrease and e/d_i increases. The highest heat transfer enhancement with only corrugations was obtained by the tubes in [83,84]. The two tubes in the investigations both have higher ratio of e/d_i and lower ratio of p/d_i. Heat transfer enhanced ratio for other tubes with only corrugations are all within 2.0. The reason of lower heat transfer enhancement ratio is caused by lower thermal conductivity and lower heat transfer coefficient of gases. It is effective for reducing resistance with alternating elliptical tubes [85]. Under the identical pumping power, Nu of alternating elliptical tube is about 84–134% higher than that of a circular smooth tube.

The solid curves in Figs. 13 and 14 show the Nu/Pr^n and f against Reynolds number for tubes with corrugations. The slope of Nu and

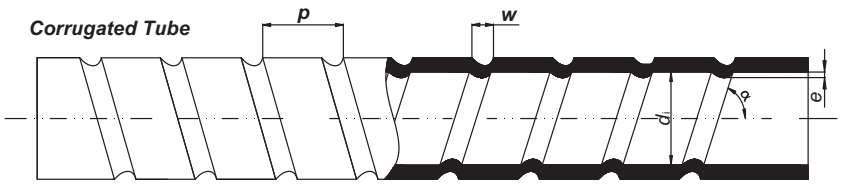

Fig. 12. Schematic diagram of corrugated tubes.

Table 4
Experimental data for tubes with corrugations.

Investigators	*Re*	Fluid	Tube/number	Best tube/feature	f/f_p	Nu/Nu_p
Kidd [89]	$20–260 \times 10^3$	Air	Corrugated/9	$p/d_i = 0.8$, $e/d_i = 0.037$	1.6–1.7	1.3–1.5
Obot et al. [83]	$0.7–50 \times 10^3$	Air	Corrugated/3	$p/d_i = 0.2$, $e/d_i = 0.056$	2.7–3.6	1.6–2.2
Esen et al. [84]	$0.6–44 \times 10^3$	Air	Corrugated/23	$p/d_i = 0.522$, $e/d_i = 0.066$	2.7–3.6	1.7–2.3
Wu et al. [86]	$10–80 \times 10^3$	Air	Corrugated tube with inlet vane swirl promoter/18	Cross spiral, $p/d_i = 0.567$, $e/d_i = 0.031$, 5#swirler	8.3–9.6	2.5–3.0
Abedin and Lampinen [90]	$0.4–4.5 \times 10^3$	Air	Corrugated tube/1	$e/d_i = 0.02$, $\alpha = 18°$	–	1.1–1.5
Li et al. [85]	$8–50 \times 10^3$	Air	Alternating elliptical tube/1	$p/d_i = 2.94$	1.75–1.9	1.6–1.9
Bilen et al. [91]	$10–38 \times 10^3$	Air	Wavy/3	$p/d_i = 0.333$, $e/d_i = 0.083$	1.8–3.0	1.4–1.7
Promvonge et al. [87]	$5–22 \times 10^3$	Air	Wavy tube with winglet vortex generators/6	$p/d_i = 1.33$, $e/d_i = 0.13$, In-line attack angle: 60°	4.6–6.2	2.4–2.7
Han et al. [92] (Simulation)	$20–70 \times 10^3$	N_2, He	Corrugated/3	$p/d_i = 2$, $e/d_i = 0.25$	1.5–1.8	1.3–1.6
Poredos et al. [88]	$2–12 \times 10^3$	Air	Corrugated/7	Corrugation ratio = 1.401	7.2–9.4	1.7–1.9
Mokkapati and Lin [93]	$40–77 \times 10^3$	Exhaust gases	Corrugated tube with twisted tape/9	$p/d_i = 0.103$, $y = 1.5$	–	1.4–1.8
Nelly et al. [94]	$4–20 \times 10^3$	Air	Corrugated tube/7	$p/d_i = 0.34$, $e/d_i = 0.043$	4.0–5.4	1.6–1.8
Han et al. [95] (Simulation)	$10–70 \times 10^3$	He	Corrugated tube/5	$p/d_i = 1.2$, $e/d_i = 0.06$	2.0–2.2	1.3–1.8
Harleβ et al. [96]	$5–23 \times 10^3$	Air	Corrugated tube/18	$p/d_i = 0.8$, $e/d_i = 0.046$	2.8–3.7	1.8–2.0

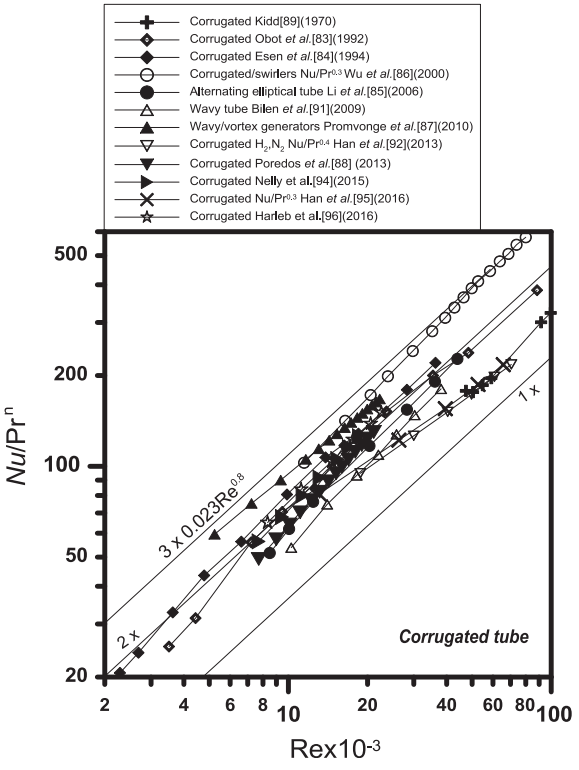

Fig. 13. Nu/Pr^n versus *Re* for corrugated tubes.

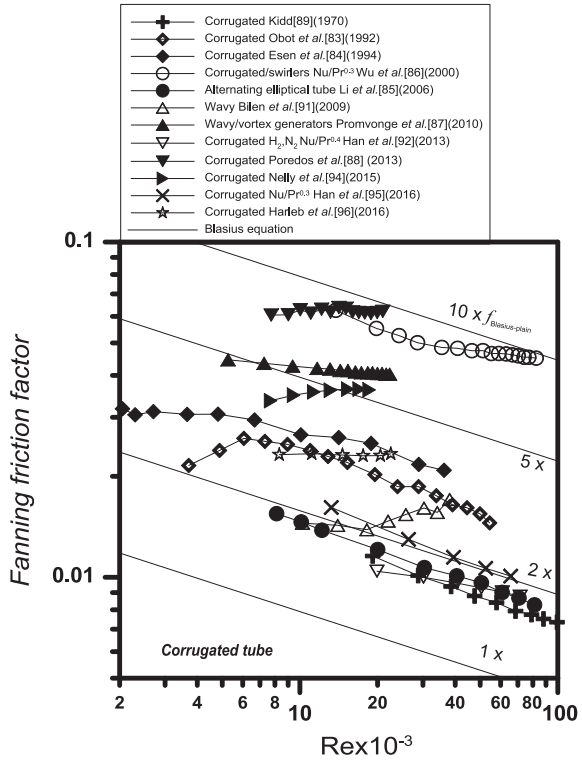

Fig. 14. Fanning friction factor versus *Re* for corrugated tubes.

friction factor with increasing Re are all similar like smooth tubes. For twelve tubes presented in the figure, two tubes with vortex generators [86,87] have the highest heat transfer coefficient. While, these two tubes also have higher pressure drop as depicted in Fig. 14. The heat transfer enhanced ratio for other tubes is typically from 1.5 to 2.0. Tubes in [88] were manufactured from aluminum strip of thickness 0.1 mm that was rolled and connected with air-tight overlay joint. The mechanism should be different

from others, which had the highest friction factor. Corrugated tubes with other forms have the pressure drop ranged from 1.6 to 5.0.

4.3. Thermal-hydraulic performance evaluation of corrugated tubes

Fig. 15 shows the performance evaluation plot of corrugated tubes in Reynolds number 2–100 × 10^3. By using corrugated tubes the heat transfer is increased by 40–230%. Except the experimental results in [88] located in Region 2, most of the experimental data located in Region 3. Heat transfer is enhanced per identical pressure drop in Region 3. The pressure drop in corrugated tubes is 1.3–10.0 times higher than in smooth tube. The compound enhancement method has higher friction factor ratio. According to the plot, alternating elliptical tube in [85] might be most effective in thermal-hydraulic performance.

Generally, most of experimental data located in the midspan position of Region 3. Moreover, for the twisted tape inserts, most of data in Region 3 are very close to the boundary of Region 2 and 3, in the lower part of Region 3. Generally, pressure drop for corrugated tubes was at the intermediate position between tubes with twisted tape inserts and internal finned tubes. More enhancement might possibly be achieved with further optimization.

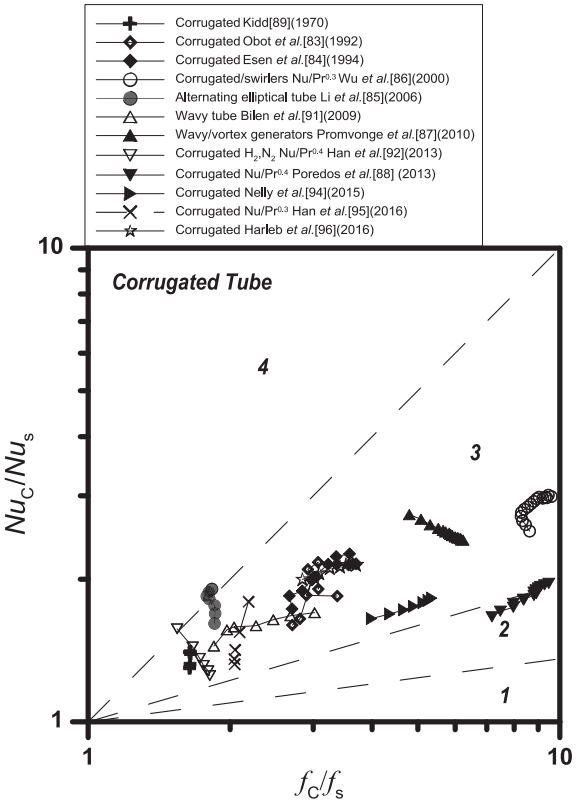

Fig. 15. Performance evaluation plot for corrugated tubes.

5. Dimpled and three dimensional roughed tubes

5.1. Introduction of dimpled and three dimensional roughed tubes

The heat transfer enhancement of three-dimensional roughed surfaces include surface roughness, dimples [97,98], protrusions and wall protuberances (see Fig. 16). Surface roughness is one of the oldest and most commonly used methods to improve the heat transfer performance in single phase convective heat transfer applications. A strong flow instabilities and fluctuation were observed after the protrusions. Integral roughness may be produced by traditional manufacturing processes such as machining, forming, casting, blasting, or welding. Most of roughness also involves the increment of surface area. Roughness also plays like fins and promotes the turbulence inside the tubes. The roughness shape has various effect in turbulence generation. Different kinds of surface roughness usually behaves differently. For the tubes with protrusions, the heat transfer and pressure drop are affected by protrusion ratio (e/d_i, the ratio of protrusion height to internal diameter). The average transverse and axis pitch of protrusions (p_t and p_a) (see Fig. 17). Because the heat transfer enhancement of gas usually need more heat transfer area, there are relatively few experimental investigations on the surface roughness with very tiny protrusions.

5.2. Experimental measurements

Experimental investigations on the tubes with dimples or three dimensional protrusions are summarized in Table 5. It is found that dimpled and roughed tubes are less frequently used in the gas heat transfer enhancement. Totally 35 tubes are reviewed and the best preformed tube in each paper is listed in the table. All the experiments were conducted in the turbulent flow with air as test fluids. The ratios of p/d_i and e/d_i are in the range of 0.5–5.26 and 0.02–0.16, respectively. The tube from Gowen and Smith [99] has the heat transfer enhanced ratios of 3.3. Dimpled tube with twisted tape in Thianpong et al. [13] has the highest increase of heat transfer and pressure drop. With single effects of dimples, the tube in Bunker and Donnellan [100] has the highest friction factor of 5.6–7.4.

Nusselt number modified by Prandtl number for dimpled tubes are shown in Fig. 18. The tube with twisted tape inserts in [13] yield the best heat transfer performance. A little bit increase of enhanced ratio is observed for the tube as the increment of Reynolds number. It is followed by the tube with sand roughed surface in [99]. The tubes in [98–100] have the heat transfer enhanced

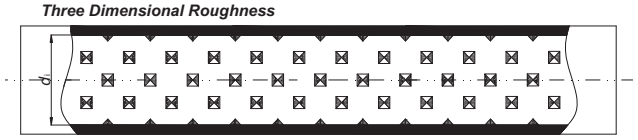

Fig. 17. Schematic diagram of three dimensional roughed tubes.

Fig. 16. Tubes with dimples.

Table 5
Experimental data for dimpled and three dimensional roughed tubes.

Investigators	*Re*	Fluid	Tube/number	Best tube /feature	f/f_p	Nu/Nu_p
Gowen and Smith [99]	$6–100 \times 10^3$	Air	Sand roughness/8	$e/d_i = 0.026$	3.4–4.8	2.3–3.3
Olsson and Sunden [101]	$0.5–6 \times 10^3$	Air	Dimpled/5	$p/d_i = 1.708$, $e/d_i = 0.16$	3.6–3.7	1.7–2.0
Bunker and Donnellan [100]	$20–50 \times 10^3$	Air	Dimpled/6	$e/d_i = 0.107$	5.6–7.4	1.9–2.1
Thianpong et al. [13]	$12–44 \times 10^3$	Air	Dimpled with tape inserts/6	$p/d_i = 0.7$, $e/d_i = 0.097$, y = 3	7.0–8.4	3.3–4.2
Wang et al. [103]	$16–50 \times 10^3$	Air	Dimpled/2	$p/d_i = 0.526$, $e/d_i = 0.053$, staggered	4.2–4.5	1.2–1.3
Wang et al. [102]	$1–70 \times 10^3$	Air	Dimpled/2	$p/d_i = 0.75$, $e/d_i = 0.075$, Ellipsoidal	1.4–1.5	1.6–2.5
Banekar et al. [110]	$3–6 \times 10^3$	Air	Almond shape dimpled /2	$p/d_i = 5.26$, $e/d_i = 0.158$	–	1.3–1.4
Apet and Borse [111]	$5–12 \times 10^3$	Air	Dimpled /4	Tube 3	–	1.5–1.6

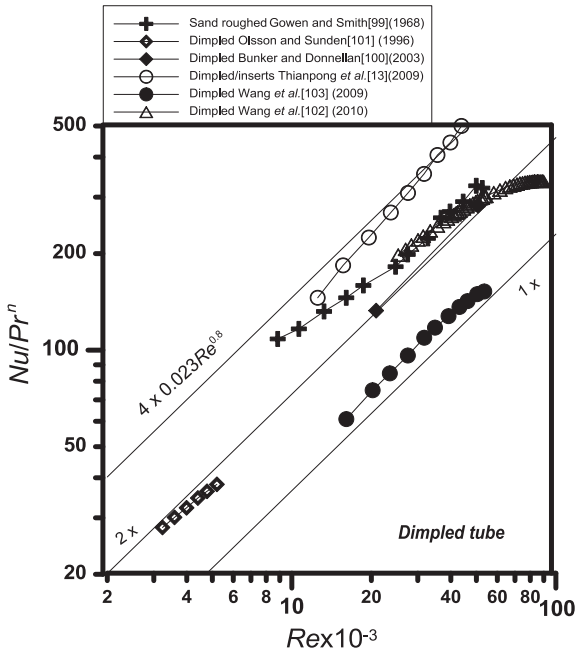

Fig. 18. Nu/Pr^n versus *Re* for dimpled tubes.

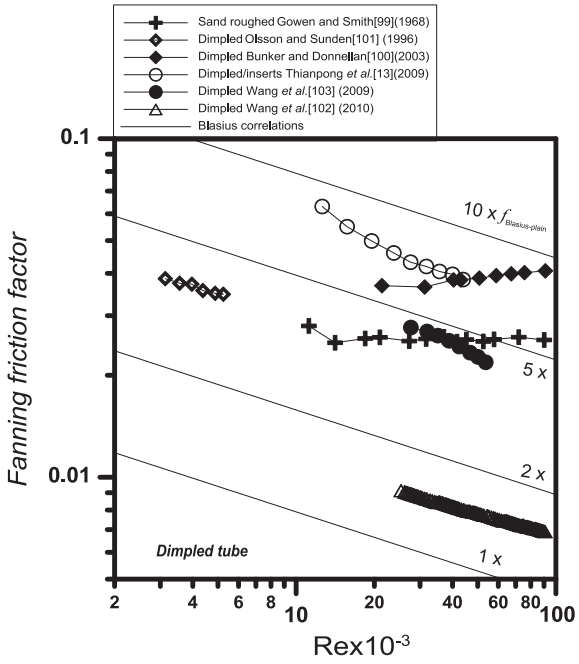

Fig. 19. Fanning friction factor versus *Re* for dimpled tubes.

ratio about 2.0. e/d_i in [103] is the lowest, which has the lowest heat transfer enhanced ratio of 1.2–1.3.

The friction factor of tubes with internal projections over Blasius equation are shown in Fig. 19. The pressure drop penalty for dimpled tube with twisted tape inserts [13] is the largest. An increment of 500–700% is observed for dimpled tube in [100]. The tubes in [99,101,103] have the friction factor ratio ranged from 3.5 to 5.0. It is observed that dimpled tubes with gas in the present investigation had the overall pressure drop ratio in the range of 3–8. It is within 5 for liquid [6].

Dimples were also used in square, rectangle and other ducts [104–109]. The application background is internal cooling passages of turbine blades and vanes, electronics, and combustion-chamber liners. The reason for heat transfer enhancement of dimpled elements is increment in the intensity and strengths of vortices, as well as increases in the magnitudes of three-dimensional turbulence. In particular, the external recirculation zone and subsequent formation of a slag layer on the wall, formed after the protrusions also contributes an important part to the heat transfer. Increase of density and height of dimples may intensify the heat transfer while accompanying with additional pressure losses.

5.3. Thermal-hydraulic performance evaluation of dimpled and three dimensional roughed tubes

The evaluation plot for dimpled and three-dimensional protrusions is shown in Fig. 20. As show in the figure, the ratio of friction factor is mostly from 1.5 to 9.0, and heat transfer enhanced ratio ranges from 1 to 4. The experimental data are mostly in Region 3, where the enhanced surface presents higher heat transfer rate than the reference one under identical pressure drop. Except the tube in [102], all the dimpled and three dimensional roughed tubes have friction factor enhanced ratios higher than 3 and heat transfer enhanced ratios are mostly within 3.

For the thermal properties such as thermal conductivity, density, Prandtl number, and dynamic viscosity, the difference between gas and liquid is basically more than an order of magnitude. The fin efficiency is typically higher for gas. The thermal resistance in convection for gases is also pretty higher than liquid or that in conduction. For instance, Nusselt number is 150 according to the survey; internal diameter of tube is 23 mm; thermal conductivity of gas is 0.0259 W/m K. The heat transfer coefficient should be 168.9 W/m^2 K. When thermal conductivity of tube wall is 236 W/m K, Biot number is 0.016. When it is 80 W/m K, Biot number is 0.049. Therefore, the thermal resistance of gas plays a predominant role in the overall heat transfer.

It is well known that for a specific three dimensional roughed tube, if the velocity is the same for air and water, the friction factor of air should be larger than water [112]. Furthermore, the friction factor increased ratio of gases are also found to be higher than liquid according the survey. For internally finned tubes, only a very small portion of experimental data located in region 4 for gases. For the tubes with twisted tape inserts, the friction factor ratio of

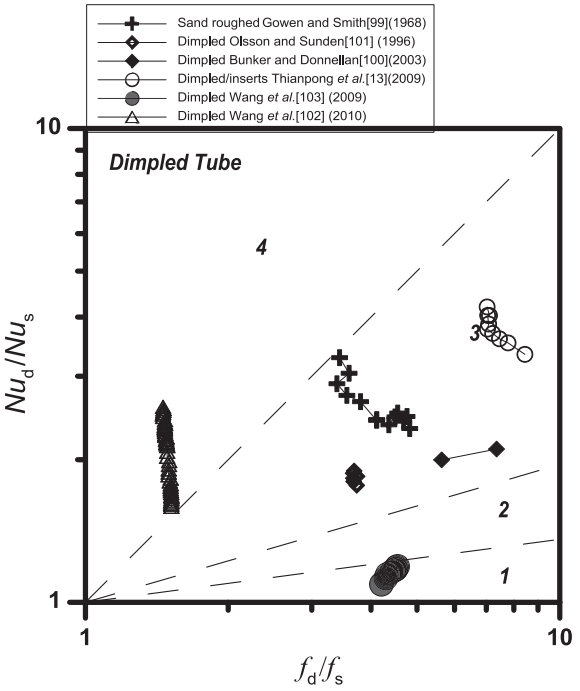

Fig. 20. Performance evaluation plot for dimpled tubes.

liquid is less than 20, while the largest ratio is more than 200 for gas. Most of experimental data located in Region 3 for liquid in corrugated tubes, while the data for gases mostly located in the lower part of Region 3. For dimpled tubes, the friction factor ratios of gases are also higher than liquids. Generally, for the above mentioned four enhancement techniques, the overall thermal efficiency of liquid is better than gases. Although the heat transfer enhanced ratios of gases normally have the same order of magnitude as liquids, the pressure drop penalties are higher.

The heat transfer enhancement of gases usually occurs in outside of tubes and involves larger heat transfer area such as continuous flat fin, wavy fin and strip fin to promote the fluid mixing. Using air as the heat transfer medium is featured by lower cost, simple system and easy maintenance. Most of the studies have been investigating the heat transfer augmentation outside of tubes. There are relatively few studies on the heat transfer of gases in tube side. The summary and evaluation in this paper give a deep insight into the heat transfer enhancement techniques inside the tubes. It is quite useful for designers of heat exchangers.

In this paper, the friction factor and Nusselt number of enhanced tubes are presented. It should be noted that the experimental data presented in the evaluation plot are from the tube which gives the best heat transfer performance in each paper. Thus, some other tubes with lower levels of heat transfer enhancement may locate in different regions of evaluation plot.

6. Conclusions

In this paper, a comprehensive survey and evaluation on the thermal-hydraulic performance of gases inside four typical enhanced techniques: internal fins, twisted tapes and swirl generators inserts, corrugations, dimples and three dimensional roughness are carried out. The evaluations on compound techniques, which involve two or more techniques utilized simultaneously are also conducted. The heat transfer and friction factor enhanced ratios of different types of enhanced techniques are presented in a same graphs with Re as the abscissa. A performance evaluation plot is adopted to identify at what constraint the studied techniques can intensify the heat transfer. And the best parameters for each types of enhanced techniques are selected. The following major conclusions are summarized as follows:

(1) The ratios of Nusselt number over Dittus-Boelter equation for internally finned tubes are typically in the range of 1–6, tubes with twisted tape inserts are 1.5–6, corrugated tubes are 1–3 and dimpled tubes are 1–4, including compound techniques. The ratios of friction factors over Blasius equation are normally in the range of 1.5–14 for internal finned tubes, 2–200 for inserted twisted tapes, corrugated tubes is 1.5–10 and dimpled tubes is 1–8.
(2) The heat transfer enhancement ratios for the gases are very similar with liquid, while the pressure drop penalties for gases are considerably higher than that for liquids. The reason for the fact is thermal properties and its own features in heat transfer. To augment the heat transfer, it might consumes more power to drive the gas.
(3) The number of investigations on the tubes fitted with twisted tapes, coil loops, and swirl generators are the largest. The pressure drop of twisted tape inserts increased appreciably at the turbulent flow compared with liquids. In the performance evaluation plot, most of data fall into the Regions of 2 and 3. The efficiency are lower compared with other three enhancement techniques in this survey.
(4) Experimental data of finned, corrugated and dimpled tubes are regularly located in Region 3, where the enhanced heat transfer can be obtained with the identical pressure drop.
(5) In the Reynolds number of 2×10^3 to 100×10^3, the tubes with internally fin in Layek et al. [22], twisted tape inserts in Bhuiya et al. [56], corrugations in Li et al. [85], and dimples in Wang et al. [102] have superior thermo-hydraulic performance over other tubes in each category.

Acknowledgement

This work was supported by the National Key Research and Development Program of China (2016YFB0601204).

References

[1] M. Benhammou, B. Draoui, M. Zerrouki, Y. Marif, Performance analysis of an earth-to-air heat exchanger assisted by a wind tower for passive cooling of buildings in arid and hot climate, Energy Convers. Manage. 91 (2015) 1–11.
[2] S. Barakat, A. Ramzy, A.M. Hamed, S.H. El Emam, Enhancement of gas turbine power output using earth to air heat exchanger (EAHE) cooling system, Energy Convers. Manage. 111 (2016) 137–146.
[3] F.P. Incropera, D.P. DeWitt, T.L. Bergman, A.S. Lavine, Fundamentals of Heat and Mass Transfer, John Wiley & Sons, 2011.
[4] Y.A. Cengel, A.J. Ghajar, Heat and Mass Transfer, fourth ed., McGraw-Hill, New York, 2011.
[5] R.L. Webb, E.R.G. Eckert, R.J. Goldstein, Heat transfer and friction in tubes with repeated-rib roughness, Int. J. Heat Mass Transfer 14 (4) (1971) 601–617.
[6] W.T. Ji, A.M. Jacobi, Y.L. He, W.Q. Tao, Summary and evaluation on single-phase heat transfer enhancement techniques of liquid laminar and turbulent pipe flow, Int. J. Heat Mass Transfer 88 (2015) 735–754.
[7] J.F. Fan, W.K. Ding, J.F. Zhang, Y.L. He, W.Q. Tao, A performance evaluation plot of enhanced heat transfer techniques oriented for energy-saving, Int. J. Heat Mass Transfer 52 (1) (2009) 33–44.
[8] J. Vogel, J. Eaton, Combined heat transfer and fluid dynamic measurements downstream of a backward-facing step, ASME J. Heat Transfer 107 (4) (1985) 922–929.
[9] J.H. Kim, K.E. Jansen, M.K. Jensen, Analysis of heat transfer characteristics in internally finned tubes, Numer. Heat Transfer, Part A: Appl. 46 (1) (2004) 1–21.
[10] D. Ryu, D. Choi, V. Patel, Analysis of turbulent flow in channels roughened by two-dimensional ribs and three-dimensional blocks. Part I: Resistance, Int. J. Heat Fluid Flow 28 (5) (2007) 1098–1111.
[11] D. Ryu, D. Choi, V. Patel, Analysis of turbulent flow in channels roughened by two-dimensional ribs and three-dimensional blocks. Part II: Heat transfer, Int. J. Heat Fluid Flow 28 (5) (2007) 1112–1124.

[12] C.H. Liu, T.N. Chung, Forced convective heat transfer over ribs at various separation, Int. J. Heat Mass Transfer 55 (19) (2012) 5111–5119.
[13] C. Thianpong, P. Eiamsa-Ard, K. Wongcharee, S. Eiamsa-Ard, Compound heat transfer enhancement of a dimpled tube with a twisted tape swirl generator, Int. C. Heat Mass Transfer 36 (7) (2009) 698–704.
[14] J. Nikuradse, Laws of Flow in Rough Pipes, National Advisory Commission for Aeronautics, Washington, DC, USA, 1950.
[15] D.F. Dipprey, R.H. Sabersky, Heat and momentum transfer in smooth and rough tubes at various Prandtl numbers, Int. J. Heat Mass Transfer 6 (5) (1963) 329–353.
[16] J. Han, L. Glicksman, W. Rohsenow, An investigation of heat transfer and friction for rib-roughened surfaces, Int. J. Heat Mass Transfer 21 (8) (1978) 1143–1156.
[17] B. Kader, A. Yaglom, Turbulent heat and mass transfer from a wall with parallel roughness ridges, Int. J. Heat Mass Transfer 20 (4) (1977) 345–357.
[18] D.L. Gee, R. Webb, Forced convection heat transfer in helically rib-roughened tubes, Int. J. Heat Mass Transfer 23 (8) (1980) 1127–1136.
[19] N.H. Kim, R. Webb, Analytic prediction of the friction and heat transfer for turbulent flow in axial internal fin tubes, ASME J. Heat Transfer 115 (3) (1993) 553–559.
[20] T. Carnavos, Heat transfer performance of internally finned tubes in turbulent flow, Heat Transfer Eng. 1 (4) (1980) 32–37.
[21] T.S. Ravigururajan, A.E. Bergles, Development and verification of general correlations for pressure drop and heat transfer in single-phase turbulent flow in enhanced tubes, Exp. Thermal Fluid Sci. 13 (1) (1996) 55–70.
[22] A. Layek, J. Saini, S. Solanki, Heat transfer and friction characteristics for artificially roughened ducts with compound turbulators, Int. J. Heat Mass Transfer 50 (23) (2007) 4845–4854.
[23] D.C. Zhang, W.T. Ji, W.Q. Tao, Condensation heat transfer of HFC134a on horizontal low thermal conductivity tubes, Int. C. Heat Mass Transfer 34 (8) (2007) 917–923.
[24] W.T. Ji, C.Y. Zhao, Y.L. He, G.N. Xi, W.Q. Tao, Vapor flow effect on falling film evaporation of R134a outside horizontal tube bundle, in: The 15th Int. Heat Transfer Conf., Kyoto, Japan, 2014.
[25] W.T. Ji, C.Y. Zhao, D.C. Zhang, Z.Y. Li, Y.L. He, W.Q. Tao, Condensation of R134a outside single horizontal titanium, cupronickel (B10 and B30), stainless steel and copper tubes, Int. J. Heat Mass Transfer 77 (2014) 194–201.
[26] W.T. Ji, M. Numata, Y.L. He, W.Q. Tao, Nucleate pool boiling and filmwise condensation heat transfer of R134a on the same horizontal tubes, Int. J. Heat Mass Transfer 86 (2015) 744–754.
[27] W.T. Ji, C.Y. Zhao, D.C. Zhang, S. Yoshioka, Y.L. He, W.Q. Tao, Effect of vapor flow on the falling film evaporation of R134a outside a horizontal tube bundle, Int. J. Heat Mass Transfer 92 (2016) 1171–1181.
[28] B. Yu, J. Nie, Q. Wang, W. Tao, Experimental study on the pressure drop and heat transfer characteristics of tubes with internal wave-like longitudinal fins, Heat Mass Transfer 35 (1) (1999) 65–73.
[29] E. Smithberg, F. Landis, Friction and forced convection heat-transfer characteristics in tubes with twisted tape swirl generators, ASME J. Heat Transfer 86 (1) (1964) 39–48.
[30] B. Yu, W. Tao, Pressure drop and heat transfer characteristics of turbulent flow in annular tubes with internal wave-like longitudinal fins, Heat Mass Transfer 40 (8) (2004) 643–651.
[31] H. Peng, L. Liu, X. Ling, Y. Li, Thermo-hydraulic performances of internally finned tube with a new type wave fin arrays, Appl. Therm. Eng. 98 (2016) 1174–1188.
[32] A. Islam, A. Mozumder, Forced convection heat transfer performance of an internally finned tube, J. Mech. Eng. 40 (1) (2009) 54–62.
[33] T. Carnavos, Cooling air in turbulent flow with internally finned tubes, Heat Transfer Eng. 1 (2) (1979) 41–46.
[34] J. Han, Heat transfer and friction in channels with two opposite rib-roughened walls, ASME J. Heat Transfer 106 (4) (1984) 774–781.
[35] M. Huq, A.A.-u. Huq, M.M. Rahman, Experimental measurements of heat transfer in an internally finned tube, Int. C. Heat Mass Transfer 25 (5) (1998) 619–630.
[36] J. Uddin, Study of pressure drop characteristics and heat transfer performance in an internally finned tube, M.Sc. Thesis, Dept. of Mech. Eng., BUET, Dhaka, Bangladesh, 1998.
[37] W.Q. Tao, S.S. Lu, H. Kang, M. Lin, Experimental study on developing and fully developed fluid flow and heat transfer in annular-sector ducts, J. Enhanced Heat Transfer 7 (1) (2000).
[38] E.S. Saad A, E.S. Sayed A, S. Mohamed M, Experimental study of heat transfer to flowing air inside a circular tube with longitudinal continuous and interrupted fins, J. Electron. Cool. Therm. Control, 2012 (2012)
[39] D.P. Mishra, K. Mohapatra, Thermo-fluid performance of finned and finless tube, Int. J. Interdiscip. Res. Centre 2 (2) (2016) 31–41.
[40] W.T. Ji, D.C. Zhang, N. Feng, J.F. Guo, M. Numata, G.N. Xi, W.Q. Tao, Nucleate pool boiling heat transfer of R134a and R134a-PVE lubricant mixtures on smooth and five enhanced tubes, ASME J. Heat Transfer 132 (11) (2010) 11502.
[41] W.T. Ji, D.C. Zhang, Y.L. He, W.Q. Tao, Prediction of fully developed turbulent heat transfer of internal helically ribbed tubes-An extension of Gnielinski equation, Int. J. Heat Mass Transfer 55 (4) (2011) 1375–1384.
[42] W.T. Ji, C.Y. Zhao, D.C. Zhang, Y.L. He, W.Q. Tao, Influence of condensate inundation on heat transfer of R134a condensing on three dimensional enhanced tubes and integral-fin tubes with high fin density, Appl. Therm. Eng. 38 (2012) 151–159.
[43] M.M.K. Bhuiya, A.K. Azad, M.S.U. Chowdhury, M. Saha, Heat transfer augmentation in a circular tube with perforated double counter twisted tape inserts, Int. C. Heat Mass Transfer 74 (2016) 18–26.
[44] M. Sheikholeslami, D.D. Ganji, M. Gorji-Bandpy, Experimental and numerical analysis for effects of using conical ring on turbulent flow and heat transfer in a double pipe air to water heat exchanger, Appl. Therm. Eng. 100 (2016) 805–819.
[45] M. Sheikholeslami, D. Ganji, Heat transfer improvement in a double pipe heat exchanger by means of perforated turbulators, Energy Convers. Manage. 127 (2016) 112–123.
[46] M. Sheikholeslami, D. Ganji, Heat transfer enhancement in an air to water heat exchanger with discontinuous helical turbulators; experimental and numerical studies, Energy 116 (2016) 341–352.
[47] M.T. Jamal-Abad, S. Saedodin, M. Aminy, Heat transfer in concentrated solar air-heaters filled with a porous medium with radiation effects: a perturbation solution, Renewable Energy 91 (2016) 147–154.
[48] R.M. Manglik, A.E. Bergles, Heat transfer and pressure drop correlations for twisted-tape inserts in isothermal tubes: part I—laminar flows, ASME J. Heat Transfer 115 (4) (1993) 881–889.
[49] R.M. Manglik, A.E. Bergles, Heat transfer and pressure drop correlations for twisted-tape inserts in isothermal tubes: Part II—Transition and turbulent flows, ASME J. Heat Transfer 115 (4) (1993) 890–896.
[50] S.W. Chang, T.L. Yang, J.S. Liou, Heat transfer and pressure drop in tube with broken twisted tape insert, Exp. Thermal Fluid Sci. 32 (2) (2007) 489–501.
[51] S.W. Chang, Y.J. Jan, J.S. Liou, Turbulent heat transfer and pressure drop in tube fitted with serrated twisted tape, Int. J. Therm. Sci. 46 (5) (2007) 506–518.
[52] K. Yakut, B. Sahin, Flow-induced vibration analysis of conical rings used for heat transfer enhancement in heat exchangers, Appl. Energy 78 (3) (2004) 273–288.
[53] S. Eiamsa-ard, P. Promvonge, Experimental investigation of heat transfer and friction characteristics in a circular tube fitted with V-nozzle turbulators, Int. C. Heat Mass Transfer 33 (5) (2006) 591–600.
[54] P. Promvonge, S. Eiamsa-ard, Heat transfer behaviors in a tube with combined conical-ring and twisted-tape insert, Int. C. Heat Mass Transfer 34 (7) (2007) 849–859.
[55] V. Kongkaitpaiboon, K. Nanan, S. Eiamsa-ard, Experimental investigation of heat transfer and turbulent flow friction in a tube fitted with perforated conical-rings, Int. C. Heat Mass Transfer 37 (5) (2010) 560–567.
[56] M. Bhuiya, J. Ahamed, M. Chowdhury, M. Sarkar, B. Salam, R. Saidur, H. Masjuki, M. Kalam, Heat transfer enhancement and development of correlation for turbulent flow through a tube with triple helical tape inserts, Int. C. Heat Mass Transfer 39 (1) (2012) 94–101.
[57] M. Bhuiya, M. Chowdhury, M. Saha, M. Islam, Heat transfer and friction factor characteristics in turbulent flow through a tube fitted with perforated twisted tape inserts, Int. C. Heat Mass Transfer 46 (2013) 49–57.
[58] M. Bhuiya, M. Chowdhury, M. Shahabuddin, M. Saha, L. Memon, Thermal characteristics in a heat exchanger tube fitted with triple twisted tape inserts, Int. C. Heat Mass Transfer 48 (2013) 124–132.
[59] M. Bhuiya, A. Sayem, M. Islam, M. Chowdhury, M. Shahabuddin, Performance assessment in a heat exchanger tube fitted with double counter twisted tape inserts, Int. C. Heat Mass Transfer 50 (2014) 25–33.
[60] H. Bas, V. Ozceyhan, Heat transfer enhancement in a tube with twisted tape inserts placed separately from the tube wall, Exp. Thermal Fluid Sci. 41 (2012) 51–58.
[61] M. Yilmaz, Ö. Çomakli, S. Yapici, Enhancement of heat transfer by turbulent decaying swirl flow, Energy Convers. Manage. 40 (13) (1999) 1365–1376.
[62] L. Wang, B. Sunden, Performance comparison of some tube inserts, Int. C. Heat Mass Transfer 29 (1) (2002) 45–56.
[63] M. Yilmaz, O. Comakli, S. Yapici, O.N. Sara, Heat transfer and friction characteristics in decaying swirl flow generated by different radial guide vane swirl generators, Energy Convers. Manage. 44 (2) (2003) 283–300.
[64] S. Eiamsa-ard, Y. Ploychay, S. Sripattanapipat, P. Promvong, An Experimental study of heat transfer and friction factor characteristics in a circular tube fitted with a helical tape, in: Proc. 18th Conf. Mech. Eng. Network of Thailand, 2004, p. 20.
[65] K. Yakut, B. Sahin, The effects of vortex characteristics on performance of coiled wire turbulators used for heat transfer augmentation, Appl. Therm. Eng. 24 (16) (2004) 2427–2438.
[66] S. Eiamsa-ard, P. Promvonge, Enhancement of heat transfer in a tube with regularly-spaced helical tape swirl generators, Sol. Energy 78 (4) (2005) 483–494.
[67] P. Promvonge, S. Eiamsa-ard, Heat transfer and turbulent flow friction in a circular tube fitted with conical-nozzle turbulators, Int. C. Heat Mass Transfer 34 (1) (2007) 72–82.
[68] P. Promvonge, S. Eiamsa-Ard, Heat transfer enhancement in a tube with combined conical-nozzle inserts and swirl generator, Energy Convers. Manage. 47 (18) (2006) 2867–2882.
[69] H. Mengna, D. Xianhe, K. Huang, L. Zhiwu, Compound heat transfer enhancement of a converging-diverging tube with evenly spaced twisted-tapes, Chin. J. Chem. Eng. 15 (6) (2007) 814–820.
[70] P. Promvonge, Thermal performance in circular tube fitted with coiled square wires, Energy Convers. Manage. 49 (5) (2008) 980–987.
[71] P. Promvonge, Thermal augmentation in circular tube with twisted tape and wire coil turbulators, Energy Convers. Manage. 49 (11) (2008) 2949–2955.
[72] S. Eiamsa-Ard, C. Thianpong, P. Eiamsa-Ard, P. Promvonge, Thermal characteristics in a heat exchanger tube fitted with dual twisted tape elements in tandem, Int. C. Heat Mass Transfer 37 (1) (2010) 39–46.

[73] S. Eiamsa-Ard, S. Rattanawong, P. Promvonge, Turbulent convection in round tube equipped with propeller type swirl generators, Int. C. Heat Mass Transfer 36 (4) (2009) 357–364.
[74] İ. Kurtbaş, F. Gülçimen, A. Akbulut, D. Buran, Heat transfer augmentation by swirl generators inserted into a tube with constant heat flux, Int. C. Heat Mass Transfer 36 (8) (2009) 865–871.
[75] T. Chompookham, C. Thianpong, S. Kwankaomeng, P. Promvonge, Heat transfer augmentation in a wedge-ribbed channel using winglet vortex generators, Int. C. Heat Mass Transfer 37 (2) (2010) 163–169.
[76] S. Gunes, V. Ozceyhan, O. Buyukalaca, Heat transfer enhancement in a tube with equilateral triangle cross sectioned coiled wire inserts, Exp. Thermal Fluid Sci. 34 (6) (2010) 684–691.
[77] N. Depaiwa, T. Chompookham, P. Promvonge, Thermal enhancement in a solar air heater channel using rectangular winglet vortex generators, in: Energy and Sustainable Development: Issues and Strategies (ESD), 2010 Proc. Int. Conf. IEEE, 2010, pp. 1–7.
[78] S. Eiamsa-Ard, P. Promvonge, Thermal characteristics in round tube fitted with serrated twisted tape, Appl. Therm. Eng. 30 (13) (2010) 1673–1682.
[79] S. Eiamsa-Ard, P. Nivesrangsan, S. Chokphoemphun, P. Promvonge, Influence of combined non-uniform wire coil and twisted tape inserts on thermal performance characteristics, Int. C. Heat Mass Transfer 37 (7) (2010) 850–856.
[80] S. Eiamsa-ard, P. Promvonge, Thermal characterization of turbulent tube flows over diamond-shaped elements in tandem, Int. J. Therm. Sci. 49 (6) (2010) 1051–1062.
[81] J. Ahamed, M. Wazed, S. Ahmed, Y. Nukman, T.T. Ya, M. Sarkar, Enhancement and prediction of heat transfer rate in turbulent flow through tube with perforated twisted tape inserts: a new correlation, ASME J. Heat Transfer 133 (4) (2011) 041903.
[82] S. Eiamsa-ard, K. Yongsiri, K. Nanan, C. Thianpong, Heat transfer augmentation by helically twisted tapes as swirl and turbulence promoters, Chem. Eng. Proc.: Process Intens. 60 (2012) 42–48.
[83] N. Obot, E. Esen, K. Snell, T. Rabas, Pressure drop and heat transfer characteristics for air flow through spirally fluted tubes, Int. C. Heat Mass Transfer 19 (1) (1992) 41–50.
[84] E. Esen, N. Obot, T.J. Rabas, Enhancement: Part I. Heat transfer and pressure drop results for air flow through passages with spirally-shaped roughness, J. Enhanc. Heat Transfer 1 (2) (1994).
[85] B. Li, B. Feng, Y.-L. He, W.Q. Tao, Experimental study on friction factor and numerical simulation on flow and heat transfer in an alternating elliptical axis tube, Appl. Therm. Eng. 26 (17) (2006) 2336–2344.
[86] H. Wu, H. Cheng, Q. Zhou, Compound enhanced heat transfer inside tubes by combined use of spirally corrugated tubes and inlet axial vane Swirlers, J. Enhanced Heat Transfer 7 (4) (2000).
[87] P. Promvonge, T. Chompookham, S. Kwankaomeng, C. Thianpong, Enhanced heat transfer in a triangular ribbed channel with longitudinal vortex generators, Energy Convers. Manage. 51 (6) (2010) 1242–1249.
[88] P. Poredoš, T. Šuklje, S. Medved, C. Arkar, An experimental heat-transfer study for a heat-recovery unit made of corrugated tubes, Appl. Therm. Eng. 53 (1) (2013) 49–56.
[89] G. Kidd, The heat transfer and pressure-drop characteristics of gas flow inside spirally corrugated tubes, ASME J. Heat Transfer 92 (3) (1970) 513–518.
[90] J. Abedin, M. Lampinen, Heat transfer coefficient measurements for smooth and rough tubes at low reynolds number, in: Proc. Int. Conf. Mech. Eng. ICME, Dhaka, Bangladesh, 2005.
[91] K. Bilen, M. Cetin, H. Gul, T. Balta, The investigation of groove geometry effect on heat transfer for internally grooved tubes, Appl. Therm. Eng. 29 (4) (2009) 753–761.
[92] H.Z. Han, B.X. Li, B.Y. Yu, Y.R. He, F.C. Li, Numerical study of flow and heat transfer characteristics in outward convex corrugated tubes, Int. J. Heat Mass Transfer 55 (25) (2012) 7782–7802.
[93] V. Mokkapati, C.-S. Lin, Numerical study of an exhaust heat recovery system using corrugated tube heat exchanger with twisted tape inserts, Int. C. Heat Mass Transfer 57 (2014) 53–64.
[94] S.M. Nelly, W. Nieratschker, M. Nadler, D. Raab, A. Delgado, Experimental and numerical investigation of the pressure drop and heat transfer coefficient in corrugated tubes, Chem. Eng. Technol. 38 (12) (2015) 2279–2290.
[95] H. Han, B. Li, W. Shao, Effect of flow direction for flow and heat transfer characteristics in outward convex asymmetrical corrugated tubes, Int. C. Heat Mass Transfer 92 (2016) 1236–1251.
[96] A. Harleß, E. Franz, M. Breuer, Experimental investigation of heat transfer and friction characteristic of fully developed gas flow in single-start and three-start corrugated tubes, Int. C. Heat Mass Transfer 103 (2016) 538–547.
[97] M. Li, T.S. Khan, E. Al-Hajri, Z.H. Ayub, Single phase heat transfer and pressure drop analysis of a dimpled enhanced tube, Appl. Thermal Eng. 101 (2016) 38–46.
[98] M. Li, T.S. Khan, E. Al Hajri, Z.H. Ayub, Geometric optimization for thermal–hydraulic performance of dimpled enhanced tubes for single phase flow, Appl. Thermal Eng. 103 (2016) 639–650.
[99] R. Gowen, J. Smith, Turbulent heat transfer from smooth and rough surfaces, Int. C. Heat Mass Transfer 11 (11) (1968) 1657–1674.
[100] R.S. Bunker, K.F. Donnellan, Heat transfer and friction factors for flows inside circular tubes with concavity surfaces, in: ASME Turbo Expo 2003, Collocated With the 2003 Int. Joint Power Generation Conf, ASME, 2003, pp. 21–29.
[101] C.O. Olsson, B. Sunden, Heat transfer and pressure drop characteristics of ten radiator tubes, Int. J. Heat Mass Transfer 39 (15) (1996) 3211–3220.
[102] Y. Wang, Y.L. He, Y.G. Lei, J. Zhang, Heat transfer and hydrodynamics analysis of a novel dimpled tube, Exp. Thermal Fluid Sci. 34 (8) (2010) 1273–1281.
[103] Y. Wang, Y.L. He, R. Li, Y.G. Lei, Heat transfer and friction characteristics for turbulent flow of dimpled tubes, Chem. Eng. Technol. 32 (6) (2009) 956–963.
[104] J. Han, J.S. Park, C. Lei, Heat transfer enhancement in channels with turbulence promoters, J. Eng. Gas Turb. Power 107 (3) (1985) 628–635.
[105] N. Burgess, P. Ligrani, Effects of dimple depth on channel Nusselt numbers and friction factors, ASME J. Heat Transfer 127 (8) (2005) 839–847.
[106] H. Lienhart, M. Breuer, C. Köksoy, Drag reduction by dimples?–A complementary experimental/numerical investigation, Int. J. Heat Fluid Flow 29 (3) (2008) 783–791.
[107] S. Chang, K. Chiang, T. Yang, C. Huang, Heat transfer and pressure drop in dimpled fin channels, Exp. Thermal Fluid Sci. 33 (1) (2008) 23–40.
[108] S. Chang, K. Chiang, T. Chou, Heat transfer and pressure drop in hexagonal ducts with surface dimples, Exp. Thermal Fluid Sci. 34 (8) (2010) 1172–1181.
[109] Y. Rao, C. Wan, Y. Xu, An experimental study of pressure loss and heat transfer in the pin fin-dimple channels with various dimple depths, Int. J. Heat Mass Transfer 55 (23) (2012) 6723–6733.
[110] S.R.B. Yogesh Dilip Banekar, Mayur Vasant Sandbhor, Dimple tube heat exchanger, Int. J Sci. Eng. Tech. Res. 4 (5) (2015) 1632–1635.
[111] S.L.B. Vilas Apet, Heat transfer enhancement in dimpled tubes, Int. J. Sci. Res. Dev. 3 (3) (2015) 3192–3195.
[112] L.F. Moody, Friction factors for pipe flow, Trans. ASME 66 (8) (1944) 671–684.